Optimal Dwell Time Allocation in Group Target Tracking Based on Recursive Bayesian Cramér-Rao Lower bound

Es. Zamani[1], S.M.M. Dehghan[2], I. Mohammadzaman[3], R. FatemiMofrad[4]

1. Ph.D Candid, 2, 3, 4. Associate Professor, Electrical and Computer Department, Malek Ashtar University of Technology, Tehran, Iran

Abstract

This paper presents an adaptive methodology for optimizing dwell time allocation in group target tracking. The approach formulates dwell time allocation as an optimization problem characterized by a cost function that integrates resource utilization and tracking accuracy. Enhancing the quality of observations is essential for improving tracking accuracy in the geometry and kinematics of group targets. This quality is influenced by the covariance of group target observations and the number of detected targets. This research clarifies the relationship between the covariance of group target observations and the number of detected targets concerning dwell time. Additionally, an analytical relationship is established between the Bayesian Cramér-Rao lower bound (BCRLB) and dwell time for evaluating accuracy in the geometry and kinematics of group target tracking. The proposed adaptive strategy is recursively optimized throughout the tracking cycle, demonstrating significant improvements over conventional methods. Simulation results indicate that optimal dwell time allocation can achieve a fourfold reduction in error compared to a constant dwell time approach, as well as a fivefold decrease in resource consumption relative to conventional methods that either detect all group members or employ a fixed dwell time.

Keywords: Phased array radar, Dwell time, Group target tracking, Optimal dwell time, Bayesian Cramér-Rao Lower Bound

1. Introduction

The rapid development of phased-array radar technology has enabled enhanced capabilities compared to conventional mechanical scanning radars. This type of radar can flexibly adjust the direction of the emitted wave to select the target to be illuminated and modify parameters such as transmission power, dwell time, and beam width. These features facilitate the management and optimization of radar resources, allowing for control over parameters such as dwell time, revisit time and beam width. Effective management of radar resources can enable the achievement of various objectives, including power savings, improved measurement and tracking accuracy, an increased number of tracked targets, and time savings. Consequently, where radar resources are constrained, such as multi-target tracking scenarios, proper resource planning is essential for phased array radar to track as many targets as possible while minimizing the required radar resources [1]. Resource management studies can be categorized into two groups. The first group tries to minimize resource consumption for given tracking accuracy requirements, and the second group has a power and bandwidth allocation strategy based on minimum emissions and the prevention of penetration [2]. When a target is illuminated by a radar beam during a scan period, the target reflects multiple pulses, and the number of pulses increases with increasing beam dwell time [3]. If all the returned pulses are integrated, meaning that more measurement information is available, the target-tracking performance is effectively enhanced.

Accepted by Scientia Iranica

Dwell time refers to the duration the radar spends observing a target during a single scan. Longer dwell times facilitate improved data collection, enhancing target detection and classification. Several important factors that influence the determination of dwell time include the size and signature of a target [4], clutter environmental conditions [5], beam width [6], and resolution [7][8]. In [9], the optimal allocation of dwell time in multitarget tracking, incorporating a simultaneous target search, is discussed. This approach utilizes the posterior Bayesian Cramér-Rao lower bound to ascertain the tracking quality of each target. A study [10] proposes Low Probability of Intercept-Based Collaborative Power and Bandwidth Allocation (LPI-CPBA) strategy for multi-target tracking in distributed radar networks, focusing on the optimization of resource allocation to improve tracking performance while minimizing energy consumption. Narikov et al. introduced Markov decision processes in temporal resource management for target tracking, adjusting dwell time, and revisiting time to maximize the tracked targets [11]. In [12], a joint revisit and dwell time management (JRDTM) strategy for single target tracking in phased array radar systems is proposed, utilizing the predicted Bayesian Cramer-Rao lower bound (BCRLB) to optimize the allocation of temporal resources while ensuring that the required tracking accuracy is maintained above a specified threshold. A new approach for choosing beams and distributing power for tracking multiple targets involves assigning limited beams and radar power to estimate the state of the target accurately [13]. It includes a new framework for selecting waveforms to track highly maneuverable targets in cluttered environments using a multi-model interactive probability data association algorithm. A new approach for coherent processing of multiple dwell times alongside each other for single and multiple targets, assuming a scanning pattern, transmitted waveform, and pulse train duration, which improves the Doppler separation performance and signal-to-noise ratio without increasing dwell time, was formulated in [7]. The Joint Dwell Time Allocation and Detection Threshold Optimization (JDTADTO) strategy improves resource efficiency in asynchronous Phased Array Radar Networks (PARN), effectively addressing challenges such as Measurement Origin Uncertainty and false alarms. This is achieved through the derivation of the Predicted Conditional Cramér-Rao Lower Bound (PC-CRLB) and the formulation of an optimization model, demonstrating the strategy's capability to enhance tracking precision under varying resource conditions [8].

Another challenge in target tracking is the tracking of group targets. When a large number of targets move close to each other in a coordinated manner, tracking them as individual targets consumes a large amount of resources. Developing an approach to improve the dwell time in group target tracking is a new topic that will be addressed in this study. For this purpose, a general understanding of group-target tracking methods is required. Various techniques for group-target tracking have been proposed, and some of the key methods are discussed in [14]. Owing to limited separability, group targets might exhibit a detection pattern similar to that of extended targets [15]. Additionally, a group target can be likened to an extended target, because the latter generates several measurements per time step [16]. A recursive Bayesian algorithm was introduced for group-target tracking in [17]. Thus, the collective motion of a group of targets is considered a single target. The group state is described as a random matrix, and the group center is tracked. The concept of group targets is introduced in [18] and proposed a group-tracking method with an adaptive elliptical window for group acceptance. The Second-Order Extended Kalman Filter is introduced to estimate the elliptic shape of moving extended and group objects, utilizing a parameterization based on

Accepted by Scientia Iranica

orientation and the lengths of the semi-axes [19]. This approach effectively relates individual measurements to the ellipse parameters through a multiplicative noise model. Monte Carlo methods have been used to track extended and group targets in [20] and [21]. Some studies have used multivariate stochastic differential equations to model the states of group members, and the group structure is described by a probabilistic transition model between members [22, 23]. The τ-Cardinalized Probability Hypothesis Density (τ-CPHD) filter effectively addresses the challenges of tracking dense group targets by first monitoring the overall group and subsequently extracting individual target states. This innovative approach combines group motion modeling with individual target motion models, enhancing the flexibility and applicability of tracking algorithms in real-world scenarios [24].

Dwell time refers to the duration a radar beam focuses on a target, enabling effective detection and tracking. This critical resource significantly influences the number of targets detected and the accuracy of measurements. When tracking groups of targets, dwell time is essential for maintaining accurate tracking of the group's shape and kinematics. Longer dwell times reveal more group members and reduce measurement error due to an improved signal-to-noise ratio. By leveraging this dual effect, adjusting dwell time during the filter estimation process can enhance the quality of group target tracking while optimizing radar resources. Figure 1 illustrates the impact of dwell time on group target tracking. As dwell time increases, measurement accuracy improves, and more group members are illuminated, enhancing overall tracking performance. Developing an optimal dwell time allocation for group target tracking is a novel topic addressed in this study. This study employs an explicit estimation algorithm for the shape parameters of a group, assuming an elliptical shape, using the extended Kalman filter with a multiplicative error model previously presented in [25]. An optimization problem is defined to adjust the dwell time, incorporating a cost function subject to specific constraints. The objective is to determine the optimal dwell time parameter throughout the filter steps sequentially, utilizing a recursively defined performance metric. The recursive Bayesian Cramér-Rao lower bound, which predicts the potential performance of any estimator [26], is employed to determine the cost function. The contributions of this research include deriving the cost function, defining the metric for group target tracking, and solving the optimization problem to extract the optimal dwell time during the filter steps. The Wasserstein distance metric is used to evaluate the proposed algorithm. The remainder of this paper is organized as follows: Section 2 presents group target tracking, including state modeling, measurement modeling, filter estimation, and the update cycle. Section 3 discusses optimal dwell time allocation, detailing the optimization problem configuration, recursive CRLB computation, group detection, and the group Geometric conformity metric. Simulation results and comparisons are provided in Section 4, and Section 5 concludes the paper.

2. Group Target Tracking

When multiple closely spaced objects move at the same speed or direction, they are called group targets. In this context, the collective movement of the group takes precedence over the individual movement of each component. The shape of a group target can be modeled using a specific geometric configuration. Group tracking involves estimating the kinematic parameters of the group's center and its shape. The state variables include the kinematics of the group center, orientation, and geometric parameters. Tracking the group center is similar to tracking a single target, leveraging existing dynamic modeling techniques. In this paper, a constant-speed model was used to describe

Accepted by Scientia Iranica

the movement of the group center due to its simplicity and low computational requirements. The geometry of the group target was approximated as an ellipse, characterized by its major diameter and rotation angle.

2.1. Group Target State Model

Targets that move in a coordinated manner over a short distance were tracked as a group. This approach is known as group-target tracking [27]. The group can consist of either many or few members. Some methods have employed geometric shapes to model the shape and center of the group for tracking group targets. Ellipsoid models are widely used for group-target tracking because the ellipsoid parameters provide meaningful information about the extent of the group, even in challenging scenarios involving highly maneuverable targets, high sensor noise, or limited detections. Furthermore, ellipses are mathematically more straightforward to describe than rectangles because they can be represented using an implicit equation or interpreted as a multivariate Gaussian distribution. In this approach, the group target is modeled as an ellipse characterized by the length and orientation of its semi-axes. The state variables include the kinematics of the group center and the geometric parameters of the group shape. The tracking of the group center is similar to that of a single target. Dynamic models of constant velocity, constant acceleration, and constant rotation are conventional models used in target motion modeling [28]. A constant-speed model is used to represent the movement of the group center, given its simplicity and low computational cost. The group target shape is modeled as an ellipse, characterized by the lengths of the semi-major and semi-minor axes, as well as the rotation angle of the ellipse relative to the horizontal axis. These ellipse parameters were assumed to be fixed with some uncertainty. The target dynamic model is presented in Equation (1) [25].

$$\boldsymbol{x}_k = \mathbf{F}\boldsymbol{x}_{k-1} + \boldsymbol{\omega} \tag{1}$$

$$\boldsymbol{x}_k = \left[m_{x,k}, \dot{m}_{x,k}, m_{y,k}, \dot{m}_{y,k}, \alpha_k, \lambda_{1,k}, \lambda_{2,k} \right]^T$$

$$\mathbf{F} = \begin{bmatrix} \boldsymbol{I}_2 \otimes \begin{bmatrix} 1 & T \\ 0 & 1 \end{bmatrix} & 0_{4\times 3} \\ 0_{3\times 4} & \boldsymbol{I}_3 \end{bmatrix} \tag{2}$$

$$\mathbf{Q} = \begin{bmatrix} \rho_1 \boldsymbol{I}_2 \otimes \begin{bmatrix} (T)^3/3 & (T)^2/2 \\ (T)^2/2 & (T) \end{bmatrix} & 0_{4\times 3} \\ 0_{3\times 4} & \rho_2 \boldsymbol{I}_3 \end{bmatrix}$$

where the state transition matrix is denoted as $\mathbf{F}$, and $\boldsymbol{\omega}$ is Gaussian noise with zero mean and variance $\boldsymbol{Q}$. $\boldsymbol{I}$, 0, ρ, and T denote the identity and zero matrices, the process noise level, and the revisit time, respectively. The operator $\otimes$ is the Kronecker multiplication. The state vector $\boldsymbol{x}_k$ includes variables for the position, velocity, and parameters of the group target geometry. This allows for the estimation of the center of the group, including its center position, velocity, rotation angle, and dimensions. $m_{x,k}$ and $\dot{m}_{x,k}$ are the position and speed of the group center in the x direction and $m_{y,k}$ and $\dot{m}_{y,k}$ show the position and speed of the group center in the y direction. The

Accepted by Scientia Iranica

geometric parameters for the target shape, α_k, $\lambda_{1,k}$, and $\lambda_{2,k}$, signify the rotation angle and the lengths of the two semi-axes of the ellipse, respectively. These variables are shown in Figure 2.

2.2. Group Target Measurement Model

Understanding the origin of the measurement and the nonlinear relationship between the target state and radar measurements is essential for the effective design and implementation of radar tracking filters. This understanding enables the filter to accurately estimate the target's state by integrating radar measurements with the dynamic model of the target. As the measuring sensor is a phased-array radar, the measurements comprise the range and azimuth of the target (Figure 2). These radar measurements are influenced by various sources of noise and uncertainties. The measurement noise is commonly represented as an additive Gaussian random variable with a known covariance matrix. Suppose that at time step k, a set of n_k measurements from the group is available (Figure 3).

$$\mathrm{Y}_k = \left\{ y_{k,1}, \ldots, y_{k,n_k} \right\} \tag{3}$$

Measurement modeling for a measurement $y_{k,i}$ consists of two components:

Group Extent Model: This model describes the location of the measurement origin $z_{k,i}$ on the target. This description is characterized by the spatial distribution $p(z_{k,i} \mid x_k)$, which depends on group parameters such as group position, length, and orientation.

Sensor Model: This model specifies the measurement $y_{k,i}$ described by $p(y_{k,i} \mid z_{k,i})$. The origin of measurement $z_{k,i}$ is mapped to the measurement $y_{k,i}$ using Equation (4).

$$\boldsymbol{y}_{k,i} = \boldsymbol{z}_{k,i} + \mathrm{V}_{k,i} \tag{4}$$

where $\mathrm{V}_{k,i}$ is the additive noise with zero mean and covariance $\boldsymbol{R}_k$. Each of measurements $y_{k,i}$ originates from the source $z_{k,i}$, which is modeled in Equation (5). In that $\left[m_{x,k}, m_{y,k} \right]^T$ is the position of the group's target center, $\boldsymbol{c}_k$ and $\boldsymbol{\lambda}_k$ are rotation and group size (half axis of the ellipse) respectively. $\boldsymbol{u}_k^i$ models multiplicative noise. If a Gaussian distribution is chosen, the group model takes the shape of an ellipse.

Accepted by Scientia Iranica

$$\boldsymbol{z}_{k,i} = \left[m_{x,k}, m_{y,k} \right]^T + \boldsymbol{H}_1 \left(\alpha_k, \lambda_k \right) . \boldsymbol{u}_k^i$$

$$\boldsymbol{c}_k = \begin{bmatrix} cos\alpha_k & -sin\alpha_k \\ sin\alpha_k & cos\alpha_k \end{bmatrix}$$

$$\boldsymbol{\lambda}_k = \begin{bmatrix} \lambda_{1,k} & 0 \\ 0 & \lambda_{2,k} \end{bmatrix} \qquad (5)$$

$$\boldsymbol{u}_k^i = \begin{bmatrix} u_{1,k}^i \\ u_{2,k}^i \end{bmatrix}$$

$\boldsymbol{u}_k^i = \mathrm{N}\left(0, \frac{1}{\kappa} I_2 \right)$, For elipticall shape $\kappa = 4$.

$$\boldsymbol{H}_1 \left(\alpha_k, \lambda_k \right) = \boldsymbol{c}_k . \boldsymbol{\lambda}_k$$

$\boldsymbol{H}_1 \left(\alpha_k, \lambda_k \right)$ is a non-linear function depending on the angle of rotation and the half length of the axes. The combination of the sensor model and the extent of the group yields Equation (6).

$$\boldsymbol{y}_{k,i} = \left[m_{x,k}, m_{y,k} \right]^T + \boldsymbol{H}_1 \left(\alpha_k, \lambda_k \right) . \boldsymbol{u}_k^i + \mathrm{V}_{k,i} \qquad (6)$$

The function $\boldsymbol{H}_2$ is utilized to correlate the spherical coordinates with the state vector, as shown in Equation (7).

$$\boldsymbol{H}_2 = \begin{bmatrix} Range \\ Azimut \end{bmatrix} \begin{bmatrix} \sqrt{\left(m_{x,k} - x_o \right)^2 + \left(m_{y,k} - y_o \right)^2} \\ arctan\left(\dfrac{m_{y,k} - y_o}{m_{x,k} - x_o} \right) \end{bmatrix} \qquad (7)$$

where $\left(x_o, y_o \right)$ denotes the radar position.

2.3. Filter estimation and update cycle procedures

Two stages of updating and estimation are used in the group target tracking via MEM-EKF*. The key difference lies in estimating the group geometry parameters and calculating covariance with a nonlinear Equation (6) for observations in the update phase. The explanations and relationships of the algorithm have been reviewed from various sources, including [25]. The filter stages are described in the following sections. To simplify understanding, state variables related to kinematics and geometry are separated, resulting in Equations (8) and (9) that form the dynamic model of the group target.

$$\boldsymbol{m}_k = \mathbf{F}_{\boldsymbol{m}} \boldsymbol{m}_{k-1} + \boldsymbol{\omega}_m \qquad (8)$$

$$\boldsymbol{s}_{\boldsymbol{k}} = \mathbf{F}_{\mathbf{s}} \boldsymbol{s}_{\boldsymbol{k}-1} + \boldsymbol{\omega}_{\boldsymbol{s}} \qquad (9)$$

Accepted by Scientia Iranica

where $\mathbf{F}_m$ and $\mathbf{F}_s$ are transition state matrices. $\boldsymbol{\omega}_m$ and $\boldsymbol{\omega}_s$ are the process noise with zero mean and Q_m^{ω} and Q_s^{ω} covariance matrices, respectively. $\boldsymbol{m}=\left[m_x \dot{m}_x \; m_y \; \dot{m}_y\right]^T$ and $s=\left[\alpha \; \lambda_1 \; \lambda_2\right]^T$ represents the kinematics state of the group center and geometric parameters of the group in the state vector respectively.

Update of center kinematics and group's geometry

The update stage is executed in two parts: the update of the center kinematics and the update of the group geometry. The measurements obtained at time step k, denoted by (3), are sequentially utilized in the update process. The kinematic state estimate was updated according to the Kalman filter update equations using the measurement $y_{k,i}$ (Equations 10-12).

$$\hat{\boldsymbol{y}}_{k,i}=\boldsymbol{H}_2\left(\hat{\boldsymbol{m}}_{k,i-1}\right) \tag{10}$$

$$\hat{\boldsymbol{m}}_{k,i}=\hat{\boldsymbol{m}}_{k,i-1}+\boldsymbol{P}_{k,i}^{my}\left(\boldsymbol{P}_{k,i}^{y}\right)^{-1}\left(\boldsymbol{y}_{k,i}-\hat{\boldsymbol{y}}_{k,i}\right) \tag{11}$$

$$\boldsymbol{P}_{k,i}^{m}=\boldsymbol{P}_{k,i-1}^{m}-\boldsymbol{P}_{k,i}^{my}\left(\boldsymbol{P}_{k,i}^{y}\right)^{-1}\left(\boldsymbol{P}_{k,i}^{my}\right)^{T} \tag{12}$$

where $\hat{\boldsymbol{m}}_{k,i-1}$ and $\boldsymbol{P}_{k,i-1}^{m}$ are the group center kinematic state estimation and the corresponding covariance matrix, respectively. $\boldsymbol{P}_{k,i}^{y}$ and $\boldsymbol{P}_{k,i}^{my}$ are the measurement covariance and cross covariance between the measurement and kinematic state, respectively, as described below. Measurement Equation (6) is nonlinear; therefore, to utilize the extended Kalman filter algorithm, linearization is required. For this purpose, the Jacobian $\boldsymbol{H}_1\left(\alpha_k,\lambda_k\right).\boldsymbol{u}_k^i$ should be calculated by considering u_k^i as a random variable.

$$\begin{aligned}&\boldsymbol{H}_{1k}.\boldsymbol{u}_k^i\approx\hat{\boldsymbol{H}}_{1k}^{i-1}.\boldsymbol{u}_k^i+\hat{\mathbf{J}}_k^{i-1}\left(\boldsymbol{s}_k-\hat{\boldsymbol{s}}_k^{i-1}\right)\\&\boldsymbol{H}_{1k}=\boldsymbol{H}_1\left(\alpha_k,\lambda_k\right)\\&\hat{\boldsymbol{H}}_{1k}^{i-1}=\hat{\boldsymbol{H}}_1\left(\alpha_{k,i-1},\lambda_{k,i-1}\right)\end{aligned} \tag{13}$$

where $\mathbf{J}$ is, the Jacobian of $\boldsymbol{H}_1\left(\alpha_k,\lambda_k\right).\boldsymbol{u}_k^i$.

$$\mathbf{J}=\begin{bmatrix}-\lambda_2\cos\alpha u_2-\lambda_1\sin\alpha u_1 & u_1\cos\alpha & -u_2\sin\alpha\\ \lambda_1\cos\alpha u_1-\lambda_2\sin\alpha u_2 & u_1\sin\alpha & u_2\cos\alpha\end{bmatrix} \tag{14}$$

The covariance of $\boldsymbol{H}_{1k}.\boldsymbol{u}_k^i$, is estimated by $\boldsymbol{Q}^H$.

$$\boldsymbol{Q}^H=\hat{\boldsymbol{H}}_{1k}^{i-1}\boldsymbol{Q}^u\left(\hat{\boldsymbol{H}}_{1k}^{i-1}\right)^T+\operatorname{tr}\left\{P_{k,i-1}^{s}\left(\hat{\boldsymbol{J}}_{nk}^{i-1}\right)^T\boldsymbol{Q}^u\hat{\boldsymbol{J}}_{mk}^{i-1}\right\} \quad \text{for } m,n=1,2 \tag{15}$$

Accepted by Scientia Iranica

where $\boldsymbol{Q}^{u}$ represents the covariance of the $\boldsymbol{u}_k^i$ distribution. P_k^s denotes the covariance of the geometry parameters, which is calculated at a later stage.

To update the geometry, a pseudo measurement is first performed using the Kronecker product.

$$\boldsymbol{Y}_{k,i}^{*}=\mathbf{T}\left(\left(\boldsymbol{y}_{k,i}-\hat{\boldsymbol{y}}_{k,i}\right)\otimes\left(\boldsymbol{y}_{k,i}-\hat{\boldsymbol{y}}_{k,i}\right)\right). \tag{16}$$

Matrix $\mathbf{T}$ was used to remove duplicate elements resulting from the Kronecker product operation.

$$\mathbf{T}=\begin{bmatrix}1&0&0&0\\0&0&0&1\\0&1&0&0\end{bmatrix} \tag{17}$$

The pseudo measured geometry parameters $\boldsymbol{Y}_{k,i}^{*}$ are also updated using Kalman filter update formulas (Equations (18) and (19)).

$$\hat{\boldsymbol{s}}_{k,i}=\hat{\boldsymbol{s}}_{k,i-1}+\boldsymbol{P}_{k,i}^{\boldsymbol{sY}^{*}}\left(\boldsymbol{P}_{k,i}^{\boldsymbol{Y}^{*}}\right)^{-1}\left(\boldsymbol{Y}_{k,i}^{*}-\hat{\boldsymbol{Y}}_{k,i}^{*}\right) \tag{18}$$

$$\boldsymbol{P}_{k,i}^{\boldsymbol{s}}=\boldsymbol{P}_{k,i-1}^{\boldsymbol{s}}-\boldsymbol{P}_{k,i}^{\boldsymbol{sY}^{*}}\left(\boldsymbol{P}_{k,i}^{\boldsymbol{Y}^{*}}\right)^{-1}\left(\boldsymbol{P}_{k,i}^{\boldsymbol{sY}^{*}}\right)^{T} \tag{19}$$

where $\hat{\boldsymbol{s}}_{k,i}$, $\boldsymbol{P}_{k,i}^{\boldsymbol{s}}$, $\hat{\boldsymbol{Y}}_{k,i}^{*}$, $\boldsymbol{P}_{k,i}^{\boldsymbol{Y}^{*}}$ and $\boldsymbol{P}_{k,i}^{\boldsymbol{sY}^{*}}$ are the estimated geometry parameters, the geometry parameters covariance matrix, the predicted pseudo-measurement, the pseudo-measurement covariance, and the cross covariance between the pseudo measurement and the geometry parameters, respectively. Finally, the covariance of the measurement and the cross-covariance between the measurement and kinematic state are calculated as follows:

$$\boldsymbol{P}_{k,i}^{my}=\boldsymbol{P}_{k,i-1}^{m}.\tilde{H}_2^{T} \tag{20}$$

$$\boldsymbol{P}_{k,i}^{y}=\tilde{H}_2.\boldsymbol{P}_{k,i-1}^{m}.\tilde{H}_2^{T}+\boldsymbol{Q}^{H}+\boldsymbol{R}_k\left(T_d^k\right) \tag{21}$$

Estimation of the group's center and geometry

Because the kinematic state parameters and group geometry over time follow a linear model, the estimation can be performed using the standard Kalman filter estimation relations (Equation (22-25).

$$\hat{\boldsymbol{m}}_{k+1,0}=\boldsymbol{F}_k^{m}\hat{\boldsymbol{m}}_{k,n_k} \tag{22}$$

$$\boldsymbol{P}_{k+1,0}^{m}=\boldsymbol{F}_k^{m}\boldsymbol{P}_{k,n_k}^{m}\left(\boldsymbol{F}_k^{m}\right)^{T}+Q_m^{\omega} \tag{23}$$

$$\hat{\boldsymbol{s}}_{k+1,0}=\boldsymbol{F}_k^{s}\hat{\boldsymbol{s}}_{k,n_k} \tag{24}$$

$$\boldsymbol{P}_{k+1,0}^{s}=\boldsymbol{F}_k^{s}\boldsymbol{P}_{k,n_k}^{s}\left(\boldsymbol{F}_k^{s}\right)^{T}+Q_s^{\omega} \tag{25}$$

Accepted by Scientia Iranica

In measurement update, the next measurement $y_{k,i}$ is used to obtain updated estimates of $\hat{\boldsymbol{m}}_{k,i}$, $\hat{\boldsymbol{s}}_{k,i}$, $\boldsymbol{P}_{k,i}^{m}$, and $\boldsymbol{P}_{k,i}^{s}$ is used. According to this notation, the predicted estimates are represented as zero samples.

By utilizing the aforementioned group target tracking algorithm, a criterion must be established for tracking quality. This criterion should be used to adjust the dwell time, ensuring that the tracking accuracy is maintained across different states of group target while minimizing dwell time consumption. This issue is discussed in the next section.

3. Optimal dwell time allocation

The block diagram of the optimal dwell time allocation framework for group target tracking is depicted in Figure 4. The represented block diagram is divided into three main components. The optimal dwell times are obtained by solving an optimization problem subject to the constraints of available resources and desired tracking quality requirements. These dwell times is then sent to the radar management unit to control the number of transmitted pulses. The illuminated targets from the group targets referred to as observations or measurements, are fed into the group target tracking algorithm. These observations are used to estimate the group center's kinematics and geometry. This estimation is then sent to the tracking-quality computation unit to determine the optimal dwell time for the next radar cycle. Several sophisticated group target tracking algorithms have been developed, including those leveraging Multi-Bernoulli and labeled multi-Bernoulli filters with refined state transition models [29,30], graph-theoretic approaches for group structure estimation [31], as well as Poisson multi-Bernoulli mixture and belief-propagation frameworks accounting for unresolved groups and uncertain detection probabilities [32,33]. Each of these methods incorporates unique modeling assumptions and filtering recursions tailored to specific group dynamics and measurement models. Consequently, extending our proposed Bayesian Cramér-Rao Lower Bound (BCRLB)-based optimal dwell time allocation framework to these advanced tracking algorithms requires a dedicated derivation of the corresponding performance bounds for each filter type, which involves detailed and model specific mathematical reformulations. Such derivations are beyond the current scope and represent important directions for future work. The optimal dwell time can be achieved by formulating an optimization problem that balances tracking quality and resource consumption. For this purpose, defining an appropriate criterion or metric to quantify tracking quality is necessary. The recursive Bayesian Cramér-Rao bound expresses the lower limit of the mean squared error (MSE) of any unbiased estimator of the target states. This bound is calculated based on the Fisher information matrix derived from the group observations collected during the dwell time. The cost function can be expressed as a function of dwell time by relating the dwell-time parameter to the Fisher information matrix. The objective is to identify the dwell times that minimize this cost function, thereby optimizing the balance between tracking quality—quantified by the Cramér-Rao bound—and resource consumption. Solving this optimization problem yields the optimal dwell times for each radar cycle, facilitating the best tracking performance given the available resources. The subsequent sections will discuss the evaluation of group geometry quality and the reformulation of the BCRLB based on dwell time, ultimately leading to the formulation of the optimization problem.

3.1. Assessment of Group Geometry Quality Based on Dwell Time

In group target tracking, dwell time impacts two key parameters: detection quantity and observation accuracy. Allocating excessive resources to track individual group members, especially when it is unnecessary, is inefficient,

Accepted by Scientia Iranica

particularly in large groups. Developing strategies to ensure the quality of group target tracking, even when some members are undetected, appears advantageous. Radar systems detect targets by transmitting electromagnetic waves and analyzing reflected signals. The radar receiver detects targets by comparing received signal power to a predefined threshold. The probability of detection (PD) is the likelihood that the input signal, including noise, exceeds the threshold voltage (VT). Conversely, if the signal exceeds the threshold without a target's return, it is a false alarm (PFA). The detection and false alarm criteria can be expressed as follows:

Detection: $S(t)+n(t)>V_T$

False Alarm: $n(t)>V_T$

where S(t) is the target signal, and n(t) is the noise.

The probabilities of detection and false alarms can be mathematically expressed as:

$$P_D=\int_{V_T}^{\infty}p_{s,n}(v)d_v \qquad (26)$$

$$P_{FA}=\int_{V_T}^{\infty}p_n(v)d_v \qquad (27)$$

where $p_{s,n}$ is the probability density function of voltage v in the presence of signal S and noise n, and p_n is the probability density function of voltage v in the presence of noise only.

The received signal is often represented using the in-phase (I) and quadrature phase (Q) components.

$$v=\sqrt{I^2+Q^2} \qquad (28)$$

If the in-phase (I) and quadrature phase (Q) components of the signal have Gaussian distributions, then the probability density function of the signal amplitude follows a Rayleigh distribution. The Rayleigh distribution accurately models the probability distribution of the signal amplitude in the presence of Gaussian noise, which is a common scenario in radar systems. The probability of detection in a radar system can be expressed in terms of the Marcum Q-function as [39]:

$$P_D=\mathrm{Q}_M\left(\sqrt{2\chi_N},\sqrt{-2lnP_{FA}}\right) \qquad (29)$$

where χ_N is signal to noise ratio.

Figure 5 plots the probability of detection against the signal-to-noise ratio for various false alarm probabilities. Increasing the radar dwell time on a target enhances its signal to-noise ratio, thereby improving detection probability. Dwell time control can also be used to manage the number of observations obtained from a group. As dwell times lengthen, measurement reliability improves through reduced noise, enabling more accurate target state estimation. Conversely, shorter dwell times yield noisier measurements, forcing the filter to rely more heavily on predicted states and potentially reducing estimation accuracy.

Therefore, the observation equation for group targets can be rewritten as follows:

Accepted by Scientia Iranica

$$P(\boldsymbol{y}_k \mid \boldsymbol{x}_k) = \mathrm{N}\left(\boldsymbol{y}_k; \boldsymbol{H}_2 \boldsymbol{x}_k, \frac{1}{\kappa}\boldsymbol{C}_k \boldsymbol{\lambda}_k \boldsymbol{\lambda}_k^T \boldsymbol{C}_k^T + \boldsymbol{R}_k\left(T_d^k\right)\right) \tag{30}$$

where:

$$\boldsymbol{R}_k\left(T_k^d\right) = \begin{bmatrix} \sigma_{R_k}^2 & 0 \\ 0 & \sigma_{\theta_k}^2 \end{bmatrix} \propto \begin{bmatrix} \frac{1}{SNR_k} & 0 \\ 0 & \frac{1}{SNR_k} \end{bmatrix} \tag{31}$$

Figure 6 illustrates the effects of increasing and decreasing dwell times in the four general scenarios. When the dwell time consumption is minimal, only a few observations from the group are obtained, potentially as few as zero or one. In this figure, at least one observation is assumed to exist. In this case, only one point from the group is obtained, which may be the group's center, and no information about the group's geometry is available. Therefore, the geometry of a group can be arbitrary. In the second scenario, a slight increase in dwell time yields four observations from the group. Although the spent resources do not significantly improve the desired quality of group tracking, the tracking quality is still evident compared to the previous state, and an estimate of the target geometry has been formed. In the third scenario, the dwell time was optimally allocated according to the dynamics and geometry of the group target to ensure high quality tracking. In the fourth scenario, resources are wasted as increased dwell time fails to significantly improve tracking quality, despite more group members being detected and a better match between measurements and targets.

Another point that should be considered is the criterion for evaluating the matching of the target geometry of the group and its estimation. The Euclidean distance square is a natural choice for comparing the estimate with the true (actual) value for point target tracking. The situation is quite different for a group of targets. As the criterion should also accommodate the shape of the group, there is no longer an obvious choice. For this purpose, various metrics have been proposed to measure the fit between estimated and true group geometries. One such metric is the Gaussian Wasserstein (GW) distance, which quantifies the dissimilarity between two elliptical shapes using the following relationship. In this article, this criterion is used to evaluate the proposed method.

$$d_{\mathrm{GW}}\left(\mathrm{N}_x, \mathrm{N}_{\hat{x}}\right)^2 = m_x - m_{\hat{x}}{}^2 + \mathrm{tr}\left(\Sigma_x + \Sigma_{\hat{x}} - 2\sqrt{\sqrt{\Sigma_x}\Sigma_{\hat{x}}\sqrt{\Sigma_x}}\right) \tag{32}$$

where m_x and Σ_x are the mean and covariance of the true group, and $m_{\hat{x}}$ and $\Sigma_{\hat{x}}$ are the mean and covariance of the estimated group, respectively. The square root of a matrix Σ is denoted as Γ that $\Sigma = \Gamma^T\Gamma$.

3.2. Reformulation of the BCRLB incorporating dwell time

In the context of state estimation within a recursive filter, the Bayesian Cramér Rao Lower Bound (BCRLB) is recognized as the theoretical lower limit of the mean squared error (MSE) for an unbiased Bayesian estimator. Existing BCRLB formulations and dwell time optimization strategies are primarily focused on multi target tracking, where targets are treated as individual entities with independent states. For instance, a joint dwell time and bandwidth optimization for individual multiple targets is presented in [3] to minimize total resource usage while

Accepted by Scientia Iranica

satisfying accuracy constraints. Similarly, dwell time and revisit time allocation approaches under Bayesian bounds for multi target scenarios are proposed in [9] and [12], with the aim of optimizing radar resources for separately tracked targets. Detection threshold optimization and dwell time allocation in asynchronous distributed radar networks, considering measurement origin uncertainty (MOU) for individual targets, are addressed in [8].

In contrast, group target tracking is considered in this study, where closely spaced targets are tracked as a cohesive entity. This fundamentally alters the tracking problem, as the focus is placed on estimating the collective geometry and kinematics of the group rather than separate target states. To our knowledge, this analytical treatment is the first to explicitly link the recursive Bayesian Cramér Rao bound with dwell time optimization in group target tracking contexts. The interplay between detection probability, group size, and observation quality is accommodated in the approach presented in this paper, elements that are typically absent in individual target tracking formulations. Thus, a new perspective and practical optimization framework are provided by the suggested adaptive dwell time allocation strategy, which is distinct from the existing literature focused on separate multi target tracking.

In the context of group target tracking, the diagonal elements of the BCRLB represent a lower bound on the variances of the estimated kinematic center of the group's motion, and the geometric parameters which characterize the shape and size of the group.

$$\begin{aligned} &\boldsymbol{P}_k \triangleq \mathrm{E}\left\{\left[\hat{\boldsymbol{X}}_{k|k}\left(y_k\right)-\boldsymbol{X}_k\right]\left[\hat{\boldsymbol{X}}_{k|k}\left(y_k\right)-\boldsymbol{X}_k\right]^T\right\} \\ &\left[\boldsymbol{P}_k\right]_{ii} \geq\left[\left(\mathrm{I}\left(\boldsymbol{X}_k\right)\right)^{-1}\right]_{ii} \end{aligned} \tag{33}$$

Given that the BCRLB is calculated as the inverse of the prior Bayesian information matrix (BIM), the primary step involves deriving the expression for BIM. BIM is defined as the negative expected value of the second derivative of the log posterior function with respect to state variable x (Equation 34).

$$\mathrm{I}\left(\boldsymbol{x}_k\right)=-\mathrm{E}_{x_k, y_k}\left[\frac{\partial^2}{\partial x_k^2} ln P\left(\boldsymbol{y}_k, \boldsymbol{x}_k\right)\right] \tag{34}$$

According to Bayes' theorem, the following relationship can be expressed.

$$P\left(\boldsymbol{y}_k, \boldsymbol{x}_k\right)=P\left(\boldsymbol{x}_k\right) P\left(\boldsymbol{y}_k \mid \boldsymbol{x}_k\right) \tag{35}$$

The relations derived by substituting Equation (35) into Equation (34) are presented below.

$$\mathrm{I}\left(\boldsymbol{x}_k\right)=\mathrm{I}_p\left(\boldsymbol{x}_k\right)+\mathrm{I}_r\left(\boldsymbol{x}_k\right) \tag{36}$$

where

$$\begin{cases} \mathrm{I}_p\left(\boldsymbol{x}_k\right)=-\mathrm{E}_{x_k, y_k}\left[\dfrac{\partial^2}{\partial \boldsymbol{x}_k^2} \ln\left(P\left(\boldsymbol{x}_k\right)\right)\right] \\ \mathrm{I}_r\left(\boldsymbol{x}_k\right)=-\mathrm{E}_{x_k, y_k}\left[\dfrac{\partial^2}{\partial \boldsymbol{x}_k^2} ln\left(P\left(\boldsymbol{y}_k \mid \boldsymbol{x}_k\right)\right)\right] \end{cases} \tag{37}$$

Considering the dynamic model outlined in Equations (8) and (9), the formulation of the prior information for estimating the target's center kinematics and group's geometry can be computed as follows:

Accepted by Scientia Iranica

$$\begin{cases} \mathrm{I}_p^m\left(\boldsymbol{m}_k\right)=\mathbf{D}_{m(k-1)}^{22}-\mathbf{D}_{m(k-1)}^{21}\left(\mathrm{I}\left(\boldsymbol{m}_{k-1}\right)+\mathbf{D}_{m(k-1)}^{11}\right)^{-1}\mathbf{D}_{m(k-1)}^{12} \\ \mathrm{I}_p^s\left(\boldsymbol{s}_k\right)=\mathbf{D}_{s(k-1)}^{22}-\mathbf{D}_{s(k-1)}^{21}\left(\mathrm{I}\left(\boldsymbol{s}_{k-1}\right)+\mathbf{D}_{s(k-1)}^{11}\right)^{-1}\mathbf{D}_{s(k-1)}^{12} \end{cases} \tag{38}$$

where

$$\mathbf{D}_{\bullet k-1}^{11}=\mathrm{E}_{\bullet_{k-1}\bullet_k}\left\{-\Delta_{\bullet_{k-1}}^{\bullet_k} lnp\left(\bullet_k|\ \bullet_{k-1}\right)\right\}$$

$$\mathbf{D}_{\bullet k-1}^{12}=\mathbf{D}_{\bullet k-1}^{21}=\mathrm{E}_{\bullet_{k-1}\bullet_k}\left\{-\Delta_{\bullet_k}^{\bullet_{k-1}} lnp\left(\bullet_k|\ \bullet_{k-1}\right)\right\}$$

$$\mathbf{D}_{\bullet k-1}^{22}=\mathrm{E}_{\bullet_{k-1}\bullet_k}\left\{-\Delta_{\bullet_k}^{\bullet_k} lnp\left(\bullet_k|\ \bullet_{k-1}\right)\right\}$$

- refers to the m and s indices.

Combined with the target dynamic model, it can be written as:

$$\begin{aligned} \mathrm{I}_p^m\left(\boldsymbol{m}_k\right)&=\left[\boldsymbol{Q}_{\boldsymbol{k}-1}^{\boldsymbol{m}}+\boldsymbol{F}_{k-1}^m\left(\mathrm{I}_p^m\right)^{-1}\left(\boldsymbol{m}_{k-1}\right)\left(\boldsymbol{F}_{k-1}^m\right)^T\right]^{-1} \\ \mathrm{I}_p^s\left(\boldsymbol{s}_k\right)&=\left[\boldsymbol{Q}_{\boldsymbol{k}-1}^{\boldsymbol{s}}+\boldsymbol{F}_{k-1}^s\left(\mathrm{I}_p^s\right)^{-1}\left(\boldsymbol{s}_{k-1}\right)\left(\boldsymbol{F}_{k-1}^s\right)^T\right]^{-1} \end{aligned} \tag{39}$$

The Bayesian Fisher Information Matrix (BFIM) for the observations (second Relation of (37)) can be calculated follows:

$$\begin{cases} \left[\mathrm{I}_r^m\left(\boldsymbol{m}_k\right)\right]_{ij}=-(\mathrm{e}^i)^T\tilde{\boldsymbol{H}}_{2k}^T\boldsymbol{\Sigma}_k^{-1}\tilde{\boldsymbol{H}}_{2k}\mathrm{e}^j-(\mathrm{e}^j)^T\tilde{\boldsymbol{H}}_{2k}^T\boldsymbol{\Sigma}_k^{-1}\tilde{\boldsymbol{H}}_{2k}\mathrm{e}^i \\ \left[\mathrm{I}_r^s\left(\boldsymbol{s}_k\right)\right]_{ij}=\mathrm{tr}\left(\boldsymbol{\Sigma}_k^{-1}\frac{\partial\boldsymbol{\Sigma}_k}{\partial\boldsymbol{s}_j}\boldsymbol{\Sigma}_k^{-1}\frac{\partial\boldsymbol{\Sigma}_k}{\partial\boldsymbol{s}_i}\right)+\mathrm{tr}\left(\boldsymbol{\Sigma}_k^{-1}\frac{\partial^2\boldsymbol{\Sigma}_k}{\partial\boldsymbol{s}_i\partial\boldsymbol{s}_j}\right) \end{cases} \tag{40}$$

where $\mathrm{e}^i\in\mathrm{R}^7$ be the unit vector where the i-th component equal 1, and all other elements equal 0, "tr" is trace oprator and $\boldsymbol{\Sigma}=\frac{1}{\boldsymbol{\kappa}}\boldsymbol{C}_k\boldsymbol{\lambda}_k\boldsymbol{\lambda}_k^T\boldsymbol{C}_k^T+\boldsymbol{R}_k\left(T_d^k\right)$.

The detailed steps for deriving the relationships are provided in Appendix A.

By computing the Bayesian Fisher Information Matrix for the observations according to Equation (37), the Cramér Rao lower bound can be extracted as a function of the dwell time. This allows the optimization problem to be defined in terms of the dwell time parameter. The optimization problem formulation will be presented in the next part.

3.3. Optimization Problem formulation

In this section, the optimization problem for dwell time allocation is formulated within a Quality of Service (QoS) framework. This framework aims to enhance group target tracking performance while efficiently managing radar resources. A novel strategy for route optimization and resource management is proposed in [40], which leverages graph theory, optimization algorithms, and radar resource allocation techniques to effectively track multiple targets in airborne radar systems. The joint detection threshold adjustment and power allocation strategy for improving

Accepted by Scientia Iranica

target tracking in cognitive MIMO radar systems is addressed by formulating the optimization problem as a mixed integer nonlinear programming (MINLP) problem, which is subsequently solved using a decomposition based approach [41]. Additionally, [42] formulates an optimization problem that integrates sidelobe suppression and waveform optimality criteria, employing an optimization algorithm to identify the optimal solution.

Recent advancements in QoS driven resource management for colocated MIMO radar multi target tracking have been made by Yi et al. [43] and Yuan et al. [44]. Yi et al. propose a scaled accuracy based objective function that leverages Bayesian Cramér Rao lower bounds (BCRLB) within a distributed netted MIMO radar system, utilizing covariance intersection fusion to address unknown inter node correlations. Their approach optimizes the weighted sum of individual target tracking accuracies, emphasizing per target performance priorities through a fast iterative descending algorithm for an inherently non convex problem. In parallel, Yuan et al. develop a robust power allocation methodology based on weighted unimodal task utility functions derived from per target BCRLB, facilitating graceful performance degradation under limited power. Their method achieves effective power scheduling for multiple independent targets by solving a non convex optimization problem via an iterative parallel search algorithm.

Despite these advancements, existing approaches primarily treat targets as independent entities, optimizing their tracking performances individually without explicitly modeling correlations or joint behaviors within groups of targets. In contrast, our work addresses the complexities of group target tracking, where the covariance structure and kinematic dependencies among targets significantly influence tracking accuracy. By extending the recursive BCRLB to group contexts, our cost function evaluates the collective tracking quality of target groups, integrating both group covariance and resource consumption (dwell time allocation) into a convex optimization framework. This group centric QoS approach explicitly captures spatial and dynamic interdependencies, enabling adaptive resource allocation that prioritizes group level tracking performance rather than merely aggregating single target metrics.

At each radar cycle, the following optimization problem should be solved:

$$\boldsymbol{T}_d^k = \underset{T^d}{\operatorname{argmin}} \left[tr\left\{ W_1 . C_{CRLB}\left(\mathbf{P}_k\right)\right\} + \sum_{i=1}^{n_k} W_2^i . T_d^i \right] \qquad s.t. T_d \in T \tag{41}$$

Let T be the set of possible dwell times, typically a continuous or discrete range of values determined by the problem constraints and the available hardware. The objective is to find the optimal dwell time allocation that minimizes a cost function, which considers the trade off between tracking accuracy and the amount of dwell time utilized.

where:

- $C_{CRLB}\left(P_k\right)$ is the Bayesian Cramér Rao Lower Bound (BCRLB) on the mean squared error (MSE) of the state estimate at the next time step, given the measurements up to the current time step.
- W_1 is an n×n diagonal matrix, where n is the number of state variables. The diagonal elements of W_1 are used to scale the state variables based on their relative importance and their rates of change, ensuring appropriate weighting in the cost function.

Accepted by Scientia Iranica

- W_2 is a weighting factor that determines the compromise between the importance of tracking accuracy (BCRLB) and the amount of dwell time utilized. The elements of W_2^i correspond to the weighting factors for the dwell times of each target in the group. Future research will explore giving more importance to boundary members for better results.
- "tr" is the trace of matrix.

Sequential Quadratic Programming (SQP) is a powerful optimization strategy for solving nonlinear optimization problems with constraints. The key advantage of the SQP algorithm is that it can efficiently handle nonlinear optimization problems with constraints by leveraging the quadratic approximation of the original problem. This quadratic approximation allows the algorithm to take into account the curvature of the objective function and constraints, leading to faster convergence compared to some other optimization methods. This approach has been utilized in numerous similar problems [40-41]. The pseudo code related to tracking with optimal dwell time is given in Table 1.

4. Simulation

In traditional radar design methods, the dwell time is usually seen as a fixed parameter. The chosen dwell time should meet the mission requirements and handle worst case scenarios. It must maintain detection capability within the radar's specified range, considering the minimum radar cross section of the targets. However, in other situations, such resource allocation may not be necessary. By using an adaptive dwell time strategy, a significant amount of resources can be saved. When tracking group targets, detecting all members can offer valuable information about the group, but it is not always essential. Therefore, in group target tracking, it is feasible to detect only the members that meet the tracking requirements and ignore the rest, thus saving resources. This method enables the radar system to optimize resource utilization based on specific operational needs.

4.1. Group Target Trajectory simulation

The simulation of the group target trajectory consists of two parts. The first part depicts the motion of the group centroid, known as the kinematics of the group center. The second part simulates the group geometry. In the first part, a motion trajectory involving constant velocity, constant acceleration, and rotation is considered in a two dimensional Cartesian coordinate system. The group target initiates from position [15 3] kilometers and concludes at position [7.5 9.2] kilometers. The trajectory of the group target is illustrated in Figure 7. The group geometry is represented by an ellipse with axes of [170 40] meters with a uniform distribution. Initially, the group target's direction approaches at a 90-degrees angle, followed by a change in direction towards a 45-degree angle. The route then transitions transversely (180-degree angle from east to west), followed by a rotation and a return to the initial route. The direction of the group target along the route is shown in Figure 8.

4-2- Sensitivity Analysis of Dwell Time on Tracking Performance

To clarify the subject, a sensitivity analysis investigated the relationship between tracking accuracy, measured by Wasserstein error, and dwell time for a group target scenario. Increasing the dwell time at the lower bound does not alter the number of observations but enhances the conformity of observations with the targets, resulting in reduced

Accepted by Scientia Iranica

observation error. Beyond this bound, extending the dwell time will increase the number of observations, leading to a decrease in the geometric tracking error of the group. Elevating the dwell time at the upper bound will no longer impact the number of observations from the group, only achieving minimal observation error. At this threshold, the minimum Wasserstein error is achieved with maximum resource utilization. This phenomenon was illustrated through a Monte Carlo analysis conducted 100 times, as depicted in Figure 9.

As Figure 9 shows, changes in the dwell time significantly affect the tracking error of the group target. This indicates that considering the group member conditions, the dwell time can be adjusted, and in this way, resources can be saved. Subsequently, a simulation for tracking a group of targets with a fixed dwell time and an adaptive dwell time will be present.

Selecting the largest possible dwell time is necessary for stable and accurate tracking of a group target with members having a low signal to noise ratio. Radar resources are wasted with this selection, especially when the targets have a good signal to noise ratio. Conversely, if it is necessary to conserve radar resources for other applications, the minimum dwell time should be selected. However, this selection will result in poor tracking accuracy in many target tracking scenarios. Another perspective in radar design could be to regulate the dwell time based on the group target conditions. Whenever a longer dwell time is needed to achieve the desired tracking accuracy, the dwell time is increased. In cases where the sensitivity is lower or the group target has favorable conditions for detection, the dwell time is decreased. This approach should utilize the proposed algorithm. To better understand the mentioned concepts, the following radar design approaches have been simulated and compared:

Case 1: Selecting a longer dwell time for consistent tracking performance

In this case, the radar system is designed with longer dwell time for tracking targets with lower SNR or less favorable detection conditions. The longer dwell time allows the radar to collect more data and improve the tracking accuracy for these challenging targets. This approach aims to maintain a consistent level of tracking performance across different target conditions.

Case 2: Selecting shorter dwell time for Low Probability of Intercept (LPI) or resource saving

In resource constrained scenarios, radar systems using a dwell time reduction approach may struggle to track or may track with significant errors the group targets with more challenging detection characteristics. This is because the reduced dwell time while minimizing the radar's energy emissions to align with Low Probability of Intercept (LPI) design principles or save resources for other radar applications impacts tracking performance and reduces accuracy.

Case 3: Comparative Analysis with optimized dwell time allocation in the Multi Target Tracking (MTT) approach

To highlight the benefits of the proposed adaptive dwell time allocation method for group target tracking, a comparative analysis is presented against the optimized dwell time allocation in the Multi Target Tracking approach. While resource allocation is optimized in this method for individual targets, detecting all group members is required, resulting in strict resource demands and potential inefficiencies, particularly in large or densely populated groups.

Case 4: Optimal dwell time adjustment based on group target conditions

Dynamic optimization of dwell time is based on the specific characteristics and conditions of the group target. This advanced approach allocates dwell time dynamically to achieve an optimal balance between tracking performance and resource utilization for the group.

Accepted by Scientia Iranica

4-3- Simulation of Various Dwell Time Allocation Approaches

Assuming that the dwell time is selectable in the range of $0.5 \le T_d \le 3.5$, the group target tracking algorithm has been simulated with four approaches. In Figure 10, the group target tracking using the MEM EKF* algorithm with a dwell time of 0.5 (a) and a dwell time of 3.5 (b) is shown. The right side plot in this figure demonstrates the group target tracking quality using the Wasserstein distance metric. As can be seen from Figures (10) (a) and (b), reducing the dwell time significantly increases the Wasserstein distance, indicating a decrease in the geometric tracking quality of the group target. Which dwell time value is preferred, the dwell time or the tracking error, depends on the requirements of the systems connected to the tracking system. By defining a cost function according to the desired requirements for tracking in the tracking system, the importance of the tracking error can be evaluated against the time spent. However, the critical issue is that if a fixed dwell time is selected in the design, with changes in the group target conditions, resource wastage will occur in some scenarios, and a significant reduction in tracking quality will occur in other scenarios.

To simulate group target tracking with an optimal dwell time, the code must align with Table (1), and the optimization problem (58) needs to be resolved during each filter cycle. Consequently, the group target from Section 3-1 was chosen as the reference for tracking, and the proposed algorithm was applied to it.

In this execution, the optimization problem with the cost function (58) was solved with the weighting factors $W_1 = [0.30.3333e33030], W_2 = 3 \times \boldsymbol{u}_w$, and the upper and lower bounds for the dwell time were set to 3.5 and 0.5, respectively ($0.5 \le T_d \le 3.5$). $\boldsymbol{u}_w$ is a unit vector with dimensions equal to the number of targets in each cycle.

The result of group target tracking with the optimal dwell time is shown in Figure 11. As can be seen from the figure, the Wasserstein distance error indicates an acceptable tracking quality, which is achieved with the optimal dwell time. The selected dwell time in the tracking cycle is shown in Figure 12.

Figures 13 and 14 compare total resource consumption (total dwell time) along the radar tracking cycles in optimized dwell time allocation for the MTT approach (case 3) versus the proposed adaptive group based allocation. Our method reduces allocated dwell time significantly, owing to the philosophy of tracking the group as a whole rather than all members individually. By allowing selective non detection of some members without sacrificing group tracking quality, radar resources are saved effectively.

Figures 15 and 16 illustrate the participation of targets during the trajectory in the above approaches. Due to different RCS values among group members, traditional fixed dwell time methods expend equal and high energy on all members, causing waste, particularly on high RCS targets. Optimized multi target methods improve allocation but require all detections, maintaining a high cumulative resource cost. The proposed method dynamically adapts dwell time based on group target conditions, preserving tracking accuracy while reducing energy spent on less impactful targets.

The group target tracking performance with the optimal dwell time was compared with the fixed dwell time approach using Monte Carlo analysis. The results of this analysis are presented in Table (2).

Accepted by Scientia Iranica

As shown in the table, the tracking process was executed for this specific group target scenario with different fixed dwell time choices. The mean and standard deviation of the Wasserstein distance error and the consumed time resources are provided for each selection.

The values for the proposed algorithm are also included in the last row of the table. As indicated in the table, the cost associated with the proposed method is the minimum. According to the table and for this scenario, the proposed method reduces the error by approximately 4 times compared to the resource preserving dwell time approach, and it reduces the consumed resources by up to 5 times compared to the tracking quality preserving dwell time approach.

5. Conclusion

This paper presents a novel approach for optimal dwell time allocation in group target tracking using phased array radar systems. The proposed method formulates an optimization problem to adjust the dwell time based on the recursive Bayesian Cramér Rao lower bound as the tracking quality criterion. The cost function balances the required resources and the tracking quality. The optimal dwell time is determined by addressing this optimization problem during the radar cycle, which is then utilized in the next radar cycle. It has been demonstrated that the calculated dwell time in the number of detected targets within a group, as well as the matching measurements, influences the group targets, and the related equations have been presented. This approach was evaluated by comparing it to fixed dwell time strategies utilizing the Gaussian Wasserstein distance metric. Simulation results demonstrate the effectiveness of the proposed method. Compared to the resource preserving dwell time approach, this technique achieved an approximately four fold reduction in tracking errors. Moreover, it enabled up to a five fold decrease in resource consumption compared to the tracking quality preserving fixed dwell time approach. The saved resources can be leveraged to track additional group targets or support other radar functionalities.

In future work, the authors plan to extend the proposed strategy to revisit time, another critical temporal resource of phased array radar systems. Optimizing the revisit time, in addition to the dwell time, can provide further opportunities to judiciously allocate the radar's limited temporal resources, enabling more efficient tracking of group targets while potentially freeing up capacity for other radar functions.

Appendix A.

To calculate the Fisher Information Matrix for observations, one needs the second derivative of the log likelihood function with respect to the parameters of the probability distribution.

$$\mathrm{I}_r\left(\boldsymbol{x}_k\right) = -\mathrm{E}\left[\frac{\partial^2}{\partial \boldsymbol{x}_k^2} ln\left(P\left(\boldsymbol{y}_k \mid \boldsymbol{x}_k\right)\right)\right] \quad \text{(A. 1)}$$

Accepted by Scientia Iranica

$$ln\left(P\left(\boldsymbol{y}_k \mid \boldsymbol{x}_k\right)\right)=-\frac{1}{2}\left(ln\left|2\pi\boldsymbol{\Sigma}\right|+\left(\boldsymbol{y}_k-\boldsymbol{x}_k\right)^T\boldsymbol{\Sigma}^{-1}\left(\boldsymbol{y}_k-\boldsymbol{x}_k\right)\right)$$
$$=-\frac{1}{2}\left(ln(2\pi)^2\left|\boldsymbol{\Sigma}\right|+\left(\boldsymbol{y}_k-\boldsymbol{x}_k\right)^T\boldsymbol{\Sigma}^{-1}\left(\boldsymbol{y}_k-\boldsymbol{x}_k\right)\right)$$
$$=-\frac{1}{2}\left(ln(2\pi)^2+ln\left|\boldsymbol{\Sigma}\right|+\left(\boldsymbol{y}_k-\boldsymbol{x}_k\right)^T\boldsymbol{\Sigma}^{-1}\left(\boldsymbol{y}_k-\boldsymbol{x}_k\right)\right) \quad (A.2)$$
$$=-\frac{1}{2}\left(2ln2\pi+ln\left|\boldsymbol{\Sigma}\right|+\left(\boldsymbol{y}_k-\boldsymbol{x}_k\right)^T\boldsymbol{\Sigma}^{-1}\left(\boldsymbol{y}_k-\boldsymbol{x}_k\right)\right)$$
$$=-ln2\pi-\frac{1}{2}\left(ln\left|\boldsymbol{\Sigma}\right|+\left(\boldsymbol{y}_k-\boldsymbol{x}_k\right)^T\boldsymbol{\Sigma}^{-1}\left(\boldsymbol{y}_k-\boldsymbol{x}_k\right)\right)$$

where

$$\boldsymbol{\Sigma}=\frac{1}{\kappa}\boldsymbol{C}_k\boldsymbol{\lambda}_k\boldsymbol{\lambda}_k^T\boldsymbol{C}_k^T+\boldsymbol{R}_k\left(T_d^k\right) \quad (A.3)$$

In this case $\boldsymbol{\Sigma}$ depends on state variables, thus first and second derivative of the log likelihood function is represent in Relation (45) and (46).

$$\frac{\partial}{\partial x_i}ln\left(P\left(\boldsymbol{y}_k \mid \boldsymbol{x}_k\right)\right)=tr\left(\boldsymbol{\Sigma}^{-1}\frac{\partial\boldsymbol{\Sigma}}{\partial x_i}\right)-(\mathrm{e}^i)^T\tilde{\boldsymbol{H}}_2\boldsymbol{\Sigma}^{-1}\left(\boldsymbol{y}_k-\tilde{\boldsymbol{H}}_2\boldsymbol{x}_{\boldsymbol{k}}\right)-$$
$$(\boldsymbol{y}_k-\tilde{\boldsymbol{H}}_2\boldsymbol{x}_{\boldsymbol{k}})^T\boldsymbol{\Sigma}^{-1}\tilde{\boldsymbol{H}}_2\mathrm{e}^i+(\boldsymbol{y}_k-\tilde{\boldsymbol{H}}_2\boldsymbol{x}_{\boldsymbol{k}})^T\frac{\partial\boldsymbol{\Sigma}^{-1}}{\partial x_i}\left(\boldsymbol{y}_k-\tilde{\boldsymbol{H}}_2\boldsymbol{x}_{\boldsymbol{k}}\right) \quad (A.4)$$

$$\frac{\partial^2}{\partial x_i x_j}lnP\left(\boldsymbol{y}_k|\boldsymbol{x}_{\boldsymbol{k}}\right)=\mathrm{tr}\left(\boldsymbol{\Sigma}^{-1}\frac{\partial^2\boldsymbol{\Sigma}}{\partial x_i\partial x_j}\right)-tr\left(\boldsymbol{\Sigma}^{-1}\frac{\partial\boldsymbol{\Sigma}}{\partial x_j}\boldsymbol{\Sigma}^{-1}\frac{\partial\boldsymbol{\Sigma}}{\partial x_i}\right)-$$
$$(\mathrm{e}^i)^T\tilde{\boldsymbol{H}}_2^T\frac{\partial\boldsymbol{\Sigma}^{-1}}{\partial x_j}\left(\boldsymbol{y}_k-\tilde{\boldsymbol{H}}_2\boldsymbol{x}_{\boldsymbol{k}}\right)+(\mathrm{e}^i)^T\tilde{\boldsymbol{H}}_2^T\boldsymbol{\Sigma}^{-1}\tilde{\boldsymbol{H}}\mathrm{e}^j+(\mathrm{e}^j)^T\tilde{\boldsymbol{H}}_2^T\boldsymbol{\Sigma}^{-1}\tilde{\boldsymbol{H}}_2\mathrm{e}^i-$$
$$(\boldsymbol{y}_k-\tilde{\boldsymbol{H}}_2\boldsymbol{x}_{\boldsymbol{k}})^T\frac{\partial\boldsymbol{\Sigma}^{-1}}{\partial x_j}\tilde{\boldsymbol{H}}_2\mathrm{e}^i-(\mathrm{e}^j)^T\tilde{\boldsymbol{H}}_2^T\frac{\partial\boldsymbol{\Sigma}^{-1}}{\partial x_i}\left(\boldsymbol{y}_k-\tilde{\boldsymbol{H}}_2\boldsymbol{x}_{\boldsymbol{k}}\right)- \quad (A.5)$$
$$(\boldsymbol{y}_k-\tilde{\boldsymbol{H}}_2\boldsymbol{x}_{\boldsymbol{k}})^T\frac{\partial\boldsymbol{\Sigma}^{-1}}{\partial x_i}\tilde{\boldsymbol{H}}_2\mathrm{e}^j+(\boldsymbol{y}_k-\tilde{\boldsymbol{H}}_2\boldsymbol{x}_{\boldsymbol{k}})^T\frac{\partial^2\boldsymbol{\Sigma}^{-1}}{\partial x_i\partial x_j}\left(\boldsymbol{y}_k-\tilde{\boldsymbol{H}}_2\boldsymbol{x}_{\boldsymbol{k}}\right)$$

The first two terms of Relation (46) are derived as follows.

$$\frac{\partial}{\partial\boldsymbol{x}_{\boldsymbol{j}}}\boldsymbol{tr}\left(\boldsymbol{\Sigma}^{-1}\frac{\partial\boldsymbol{\Sigma}}{\partial x_i}\right)=\boldsymbol{tr}\left(\frac{\partial\boldsymbol{\Sigma}^{-1}}{\partial\boldsymbol{x}_{\boldsymbol{j}}}\frac{\partial\boldsymbol{\Sigma}}{\partial x_i}\right)+\boldsymbol{tr}\left(\boldsymbol{\Sigma}^{-1}\frac{\partial^2\boldsymbol{\Sigma}}{\partial x_i\partial x_j}\right) \quad (A.6)$$

where

$$\frac{\partial\boldsymbol{\Sigma}^{-1}}{\partial\boldsymbol{x}_{\boldsymbol{j}}}=-\boldsymbol{\Sigma}^{-1}\frac{\partial\boldsymbol{\Sigma}}{\partial\boldsymbol{x}_{\boldsymbol{j}}}\boldsymbol{\Sigma}^{-1} \quad (A.7)$$

Thus,

$$\frac{\partial}{\partial\boldsymbol{x}_{\boldsymbol{j}}}\boldsymbol{tr}\left(\boldsymbol{\Sigma}^{-1}\frac{\partial\boldsymbol{\Sigma}}{\partial x_i}\right)=\boldsymbol{tr}\left(-\boldsymbol{\Sigma}^{-1}\frac{\partial\boldsymbol{\Sigma}}{\partial\boldsymbol{x}_{\boldsymbol{j}}}\boldsymbol{\Sigma}^{-1}\frac{\partial\boldsymbol{\Sigma}}{\partial x_i}\right)+\boldsymbol{tr}\left(\boldsymbol{\Sigma}^{-1}\frac{\partial^2\boldsymbol{\Sigma}}{\partial x_i\partial x_j}\right) \quad (A.8)$$

Accepted by Scientia Iranica

After computing the expected value of Relation (A. 5), simplifying, and separating the geometric and kinematic state variables, Relation (40) will be obtained.

Appendix B.

The cost function defined as Relation (41) is convex. This is established by noting that the term $\left(\mathrm{tr}\left\{W_1 C_{CRLB}\left(P_k\right)\right\}\right)$ is convex due to the positive definiteness of W_1 and C_{CRLB}, while the summation $\left(\sum_{i=1}^{n_k} W_2^i T_i^d\right)$ is also convex as it comprises linear combinations of positive terms. The sum of these convex functions is convex, and the feasible set T is assumed to be convex, confirming that the overall cost function is convex within the defined constraints.

Reference

[1] Bo, L., Linyu, T., Daqing, C., and Shiyang, L., "An adaptive dwell time scheduling model for phased array radar based on three-way decision," *Journal of Systems Engineering and Electronics*, vol. 31, no. 3, pp. 500–509, 2020, https://doi.org/10.23919/JSEE.2020.000030.

[2] Levy, B., Maman, L., Shvartzman, S., et al., "Coherent Multi-Dwell Processing of Un-Synchronized Dwells for High Velocity Estimation and Super-Resolution in Radar," *Remote Sensing*, vol. 15, no. 3, 2023, https://doi.org/10.3390/rs15030782.

[3] Ding, L., Shi, C., Qiu, W., et al., "Joint Dwell Time and Bandwidth Optimization for Multi-Target Tracking in Radar Network Based on Low Probability of Intercept," *Sensors*, vol. 20, no. 5, 2020, https://doi.org/10.3390/s20051269.

[4] Yan, J., Pu, W., Zhou, S., Liu, H., et al., "Optimal Resource Allocation for Asynchronous Multiple Targets Tracking in Heterogeneous Radar Networks," *IEEE Transactions on Signal Processing*, vol. 68, pp. 4055–4068, 2020, https://doi.org/10.1109/TSP.2020.3007313.

[5] Zhu, P., Liang, J., Luo, Z., et al., "Cognitive Radar Target Tracking Using Intelligent Waveforms Based on Reinforcement Learning," *IEEE Transactions on Geoscience and Remote Sensing*, vol. 61, pp. 1–15, 2023, https://doi.org/10.1109/TGRS.2023.3298355.

[6] Lu, X., Yi, W., Wang, Y., "Adaptive beam burden management for multi-target tracking in distributed radar network," *Signal Processing*, vol. 200, p. 108667, 2022, https://doi.org/10.1016/j.sigpro.2022.108667.

[7] Levy, B., Maman, L., Shvartzman, S., et al., "Coherent Multi-Dwell Processing of Un-Synchronized Dwells for High Velocity Estimation and Super-Resolution in Radar," *Remote Sensing*, vol. 15, no. 3, 2023, https://doi.org/10.3390/rs15030782.

[8] Zhang, H., Liu, W., Yang, X., "Resource saving based dwell time allocation and detection threshold optimization in an asynchronous distributed phased array radar network," *Chinese Journal of Aeronautics*, vol. 36, no. 11, pp. 311–327, 2023, https://doi.org/10.1016/j.cja.2023.06.017.

[9] Yuan, Y., Yi, W., Kong, L., "Joint tracking sequence and dwell time allocation for multi-target tracking with phased array radar," *Signal Processing*, vol. 192, p. 108374, 2022, https://doi.org/10.1016/j.sigpro.2021.108374.

Accepted by Scientia Iranica

[10] Shi, C., Ding, L., Wang, F., et al., "Low Probability of Intercept-Based Collaborative Power and Bandwidth Allocation Strategy for Multi-Target Tracking in Distributed Radar Network System," *IEEE Sensors Journal*, vol. 20, no. 12, pp. 6367–6377, 2020, https://doi.org/10.1109/JSEN.2020.2977328.

[11] Narykov, A. S., Krasnov, O. A., Yarovoy, A., "Algorithm for resource management of multiple phased array radars for target tracking," *Proceedings of the 16th International Conference on Information Fusion*, Istanbul, Turkey, 2013, pp. 1258–1264, ISBN:978-605-86311-1-3.

[12] Wang, X., Yi, W., Xie, M., et al., "Time management for target tracking based on the predicted Bayesian Cramer-Rao lower bound in phase array radar system," in *2017 20th International Conference on Information Fusion (Fusion)*, 2017, pp. 1–5. https://doi.org/10.23919/ICIF.2017.8009857.

[13] Li, X., Cheng, T., Tan, Q., "Joint Time-Space Resource Allocation and Waveform Selection for the Collocated MIMO Radar in Multiple Targets Tracking," in *2019 International Conference on Control, Automation and Information Sciences (ICCAIS)*, 2019, pp. 1–6. https://doi.org/10.1109/ICCAIS46528.2019.9074675.

[14] Mihaylova, L., Carmi, A. Y., Septier, F., et al., "Overview of Bayesian sequential Monte Carlo methods for group and extended object tracking," *Digital Signal Processing*, vol. 25, pp. 1–16, 2014, https://doi.org/10.1016/j.dsp.2013.11.006.

[15] Feldmann, M., Fränken, D., Koch, W., "Tracking of Extended Objects and Group Targets Using Random Matrices," *IEEE Transactions on Signal Processing*, vol. 59, no. 4, pp. 1409–1420, 2011, https://doi.org/10.1109/TSP.2010.2101064.

[16] Granström, K., Lundquist, C., "On the use of multiple measurement models for extended target tracking," in *Proceedings of the 16th International Conference on Information Fusion*, 2013, pp. 1534–1541, ISBN:978-605-86311-1-3.

[17] Koch, J. W., "Bayesian approach to extended object and cluster tracking using random matrices," *IEEE Transactions on Aerospace and Electronic Systems*, vol. 44, no. 3, pp. 1042–1059, 2008, https://doi.org/10.1109/TAES.2008.4655362.

[18] Huang, Q., Lu, D., He, L., et al., "Group Tracking Method with Adaptive Gate for Multiple Extended Objects Tracking," in *2019 IEEE 4th International Conference on Signal and Image Processing (ICSIP)*, 2019, pp. 773–776. https://doi.org/10.1109/SIPROCESS.2019.8868590.

[19] Yang, S., Baum, M., "Second-order extended Kalman filter for extended object and group tracking," *19th International Conference on Information Fusion (FUSION)*, Heidelberg, Germany, 2016, pp. 1178–1184, ISBN:978-1-5090-2012-6.

[20] Petrov, N., Mihaylova, L., Gning, A., et al., "A novel Sequential Monte Carlo approach for extended object tracking based on border parameterisation," *14th International Conference on Information Fusion*, Chicago, IL, USA, 2011, pp. 1–8, ISBN:978-1-4577-0267-9.

[21] Pang, S. K., Li, J., Godsill, S. J., "Detection and Tracking of Coordinated Groups," *IEEE Transactions on Aerospace and Electronic Systems*, vol. 47, no. 1, pp. 472–502, 2011, https://doi.org/10.1109/TAES.2011.5705687.

[22] Meyer, F., et al., "Message Passing Algorithms for Scalable Multitarget Tracking," *Proceedings of the IEEE*, vol. 106, no. 2, pp. 221–259, 2018, https://doi.org/10.1109/JPROC.2018.2789427.

Accepted by Scientia Iranica

[23] Gning, A., Mihaylova, L., Maskell, S., Pang, S. K., Godsill, S., "Ground target group structure and state estimation with particle filtering," *11th International Conference on Information Fusion*, Cologne, Germany, 2008, pp. 1–8, ISBN:978-3-8007-3092-6.

[24] Lu, Z., Hu, W., Liu, Y., Kirubarajan, T., "Seamless group target tracking using random finite sets," *Signal Processing*, vol. 176, p. 107683, 2020, https://doi.org/10.1016/j.sigpro.2020.107683.

[25] Yang, S., Baum, M., "Tracking the Orientation and Axes Lengths of an Elliptical Extended Object," *IEEE Transactions on Signal Processing*, vol. 67, no. 18, pp. 4720–4729, 2019, https://doi.org/10.1109/TSP.2019.2929462.

[26] Van Trees, H. L., Bell, K., editors. "Bayesian Bounds for Parameter Estimation and Nonlinear Filtering/Tracking," Wiley, New York, NY, 2007, ISBN 978-0-470-12095-8.

[27] Geng, W. D., Wang, Y. Q., Dong, Z. H., "Group-Target Tracking," Springer Nature jointly published with National Defense Industry Press, Singapore, 2016, https://doi.org/10.1007/978-981-10-1888-6.

[28] Melvin, W. L., Scheer, J. A., "Principles of Modern Radar," Vol. III: Radar Applications, SciTech, USA, 2014, ISBN: 978-1891121548.

[29] Li, G., Li, G., He, Y., "Resolvable Group Target Tracking via Multi-Bernoulli Filter and Its Application to Sensor Control Scenario," *IEEE Transactions on Signal Processing*, vol. 70, pp. 6286–6299, 2022, https://doi.org/10.1109/TSP.2023.3236158.

[30] Li, G., Li, G., He, Y., "Labeled Multi-Bernoulli Filter Based Multiple Resolvable Group Targets Tracking With Leader–Follower Model," *IEEE Transactions on Aerospace and Electronic Systems*, vol. 59, no. 5, pp. 6683–6694, Oct. 2023, https://doi.org/10.1109/TAES.2023.3276732.

[31] Liu, W., Zhu, S., Wen, C., et al., "Structure modeling and estimation of multiple resolvable group targets via graph theory and multi-Bernoulli filter," *Automatica*, vol. 89, 2018, pp. 274–289, ISSN 0005-1098, https://doi.org/10.1016/j.automatica.2017.12.004.

[32] Li, G., Li, G., He, Y., "Belief-Propagation-Based Resolvable Group Target Tracking With Unknown Detection Probability," *IEEE Transactions on Aerospace and Electronic Systems*, vol. 61, no. 2, pp. 3683–3700, April 2025, https://doi.org/10.1109/TAES.2024.3488685.

[33] Li, G., Li, G., He, Y., "PMBM-Based Unresolved-Group Object Tracking," *IEEE Transactions on Aerospace and Electronic Systems*, vol. 60, no. 4, pp. 4229–4240, Aug. 2024, https://doi.org/10.1109/TAES.2024.3373561.

[34] Barton, D. K., "Radar System Analysis and Modeling," Artech House, London, 2005, ISBN: 978-1580536813.

[35] Ding, L., Shi, C., Zhou, J., "Collaborative route optimization and resource management strategy for multi-target tracking in airborne radar system," *Digital Signal Processing*, vol. 138, p. 104051, 2023, https://doi.org/10.1016/j.dsp.2023.104051.

[36] Zhang, H., Liu, W., Fei, T., "Joint detection threshold adjustment and power allocation strategy for cognitive MIMO radar target tracking," *Digital Signal Processing*, vol. 126, p. 103379, 2022, https://doi.org/10.1016/j.dsp.2021.103379.

Accepted by Scientia Iranica

[37] Xu, L., Zhou, S., Liu, H., “Simultaneous optimization of radar waveform and mismatched filter with range and delay-Doppler sidelobes suppression,” *Digital Signal Processing*, vol. 83, pp. 346–358, 2018, https://doi.org/10.1016/j.dsp.2018.09.009.

[38] Yi, W., Yuan, Y., Hoseinnezhad, R., et al., "Resource Scheduling for Distributed Multi-Target Tracking in Netted Colocated MIMO Radar Systems," *IEEE Transactions on Signal Processing*, vol. 68, pp. 1602–1617, 2020, https://doi.org/10.1109/TSP.2020.2976587.

[39] Yuan, Y., Yi, W., Hoseinnezhad, R., et al., "Robust Power Allocation for Resource-Aware Multi-Target Tracking With Colocated MIMO Radars," *IEEE Transactions on Signal Processing*, vol. 69, pp. 443–458, 2021, https://doi.org/10.1109/TSP.2020.3047519.

[40] Jin, B., Kuang, X., Liu, S., et al., “Joint allocation of transmit power and signal bandwidth for distributed cognitive tracking radar network using cooperative game,” *Digital Signal Processing*, vol. 135, p. 103964, 2023, https://doi.org/10.1016/j.dsp.2023.103964.

[41] Huang, Z., Tang, B., Huang, C., et al., “Direct transmit waveform design to match a desired beampattern under the constant modulus constraint,” *Digital Signal Processing*, vol. 126, p. 103486, 2022, https://doi.org/10.1016/j.dsp.2022.103486.

Accepted by Scientia Iranica

captions

Figure 1: Improving Group Target Estimation Performance through Increased Dwell Time

Figure 2: Kinematics and geometry of group target

Figure 3: Modeling Group Observations with an Ellipse

Figure 4: Group target tracking block diagram with adaptive dwell time

Figure 5: probability of detection

Figure 6: Effect of Dwell Time on Observations of Group Target

Figure 7: Route of the Group Target

Figure 8: Direction of Group Target Along the Route

Figure 9: Impact of dwell time on Wasserstein's error

(a) Selecting a longer dwell time for consistent tracking performance (Case 1)

(b) Selecting shorter dwell time for Low Probability of Intercept (LPI) (Case 2)

Figure 10: Group Target Tracking (a) $T_d = 0.5$, (b) $T_d = 3.5$

Figure 11: Group Target Tracking with Optimal Dwell Time Allocation (Case 4)

Figure 12: Optimal Dwell Time for Group Target Tracking

Figure 13: Resource Consumption in optimized dwell time allocation for MTT approach (Scaled)

Figure 14: Resource Consumption in Optimal Dwell Time Allocation for Group Target Tracking (Scaled)

Figure 15: Participation of Targets in optimized dwell time allocation for MTT approach

Figure 16: Participation of Targets in Optimal Dwell Time Allocation for Group Target Tracking

Table 1: pseudo code of tracking with optimal dwell time

Table 2: Comparison of Various Dwell Time Allocation Approaches in Group Target Tracking

Figures

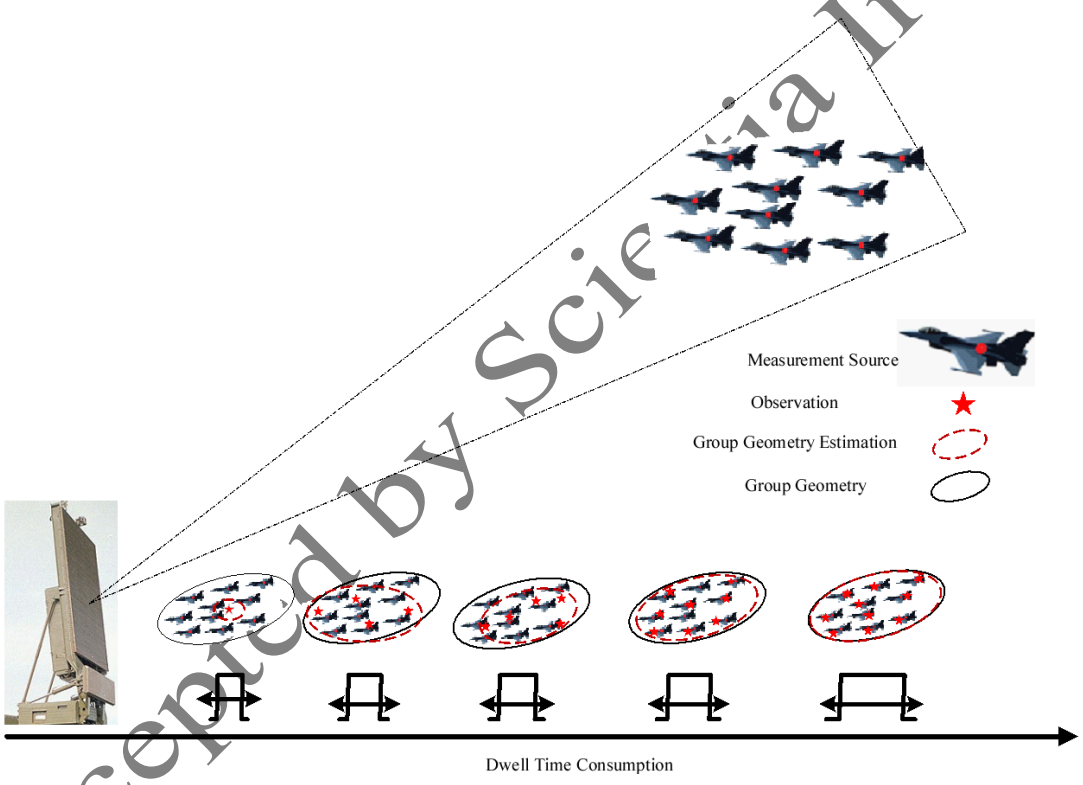

Figure 1: Improving Group Target Estimation Performance through Increased Dwell Time

Accepted by Scientia Iranica

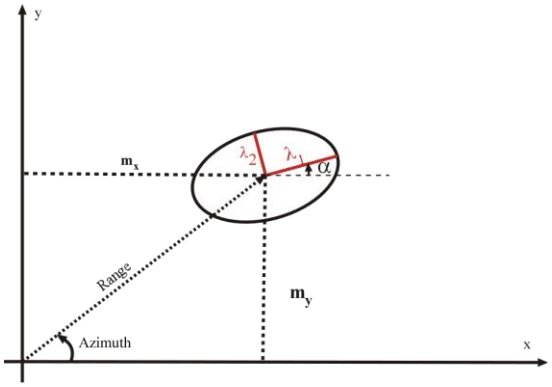

Figure 2: Kinematics and geometry of group target

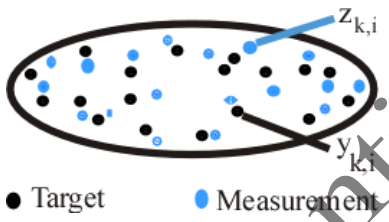

Figure 3: Modeling Group Observations with an Ellipse

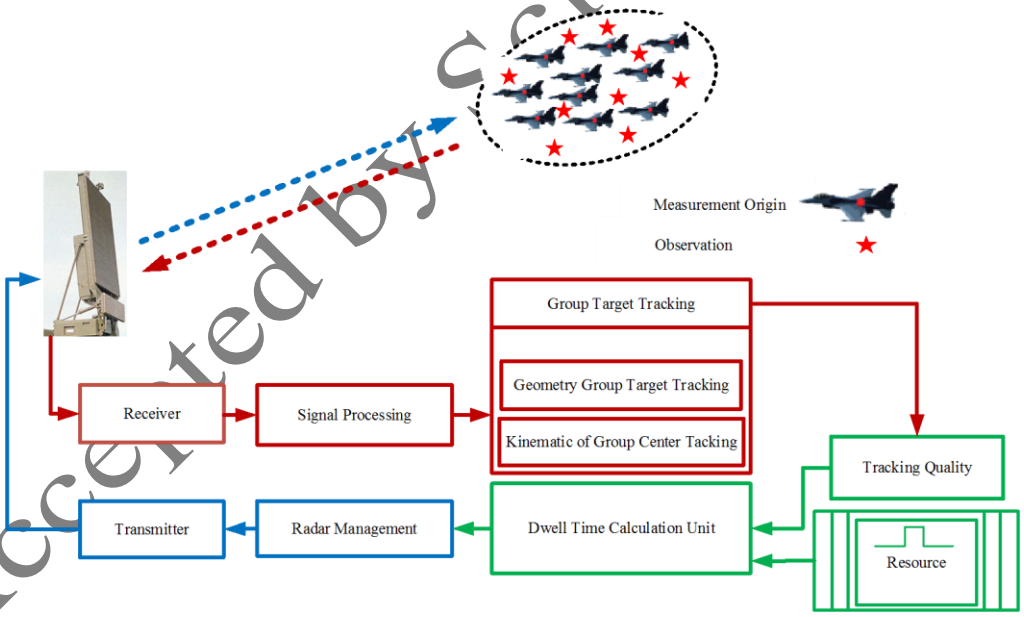

Figure 4: Group target tracking block diagram with adaptive dwell time

Accepted by Scientia Iranica

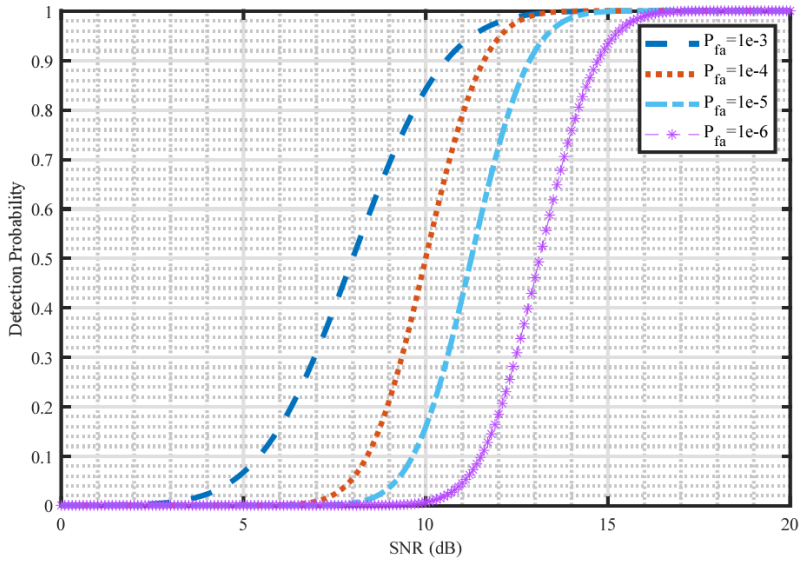

Figure 5: probability of detection

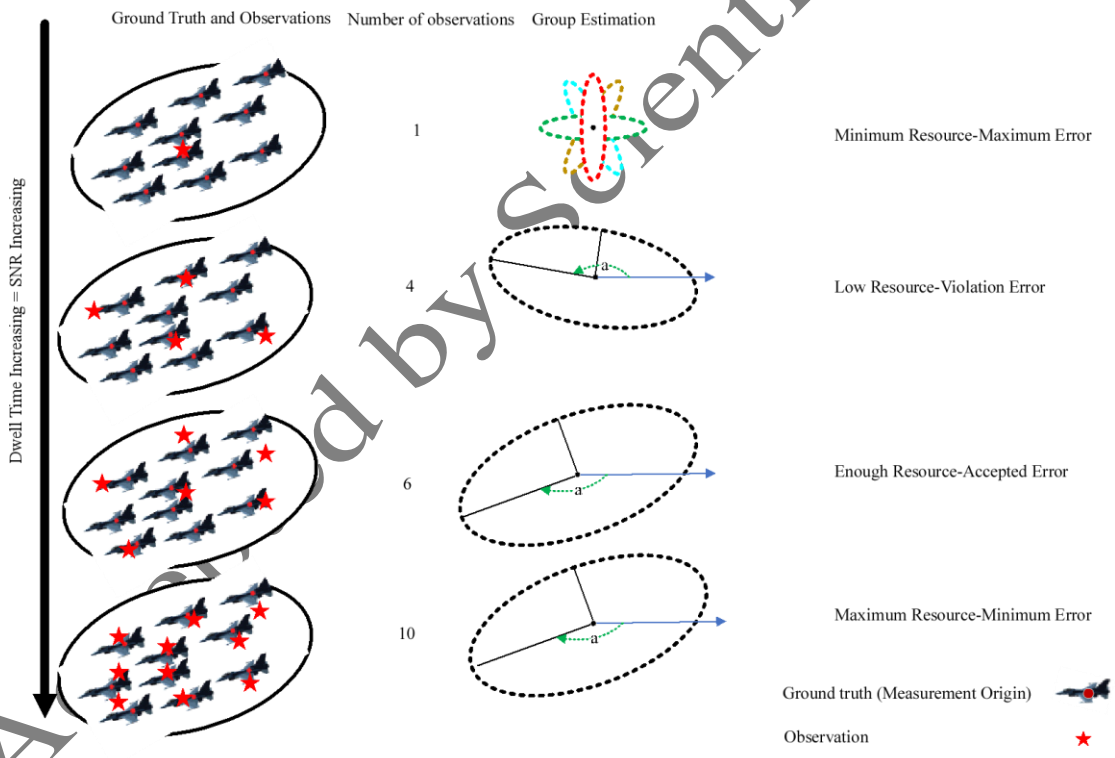

Figure 6: Effect of Dwell Time on Observations of Group Target

Accepted by Scientia

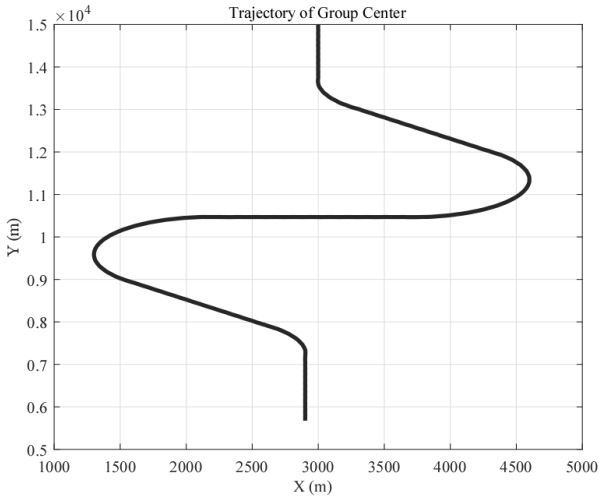

Figure 7: Route of the Group Target

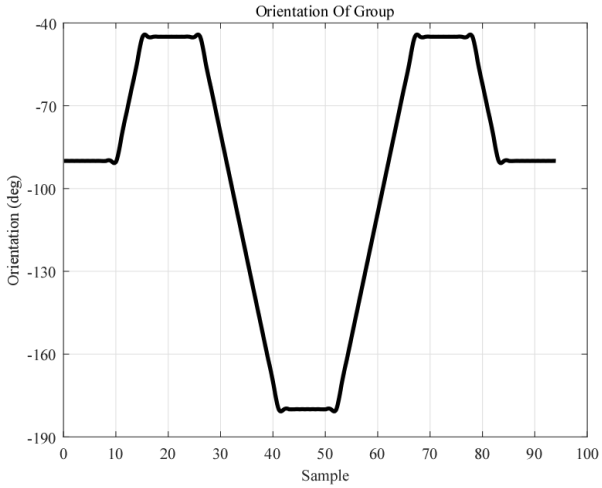

Figure 8: Direction of Group Target Along the Route

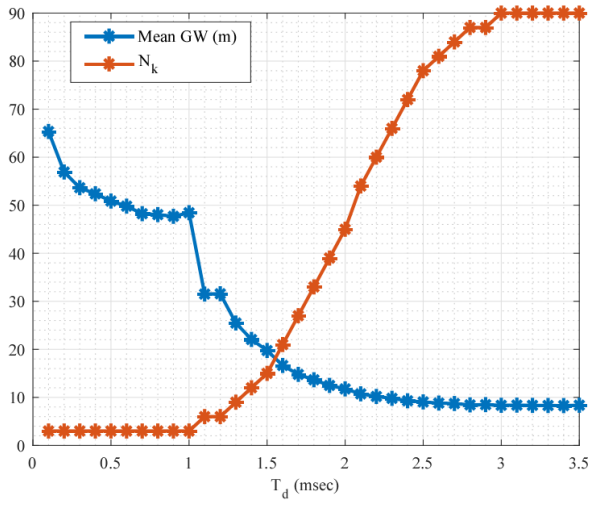

Figure 9: Impact of dwell time on Wasserstein's error

Accepted Manuscript
Iranica

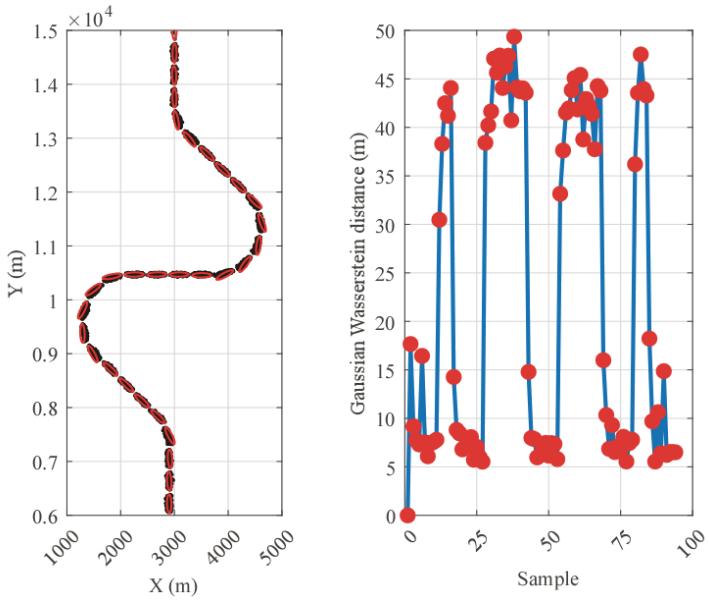

(a) Selecting a longer dwell time for consistent tracking performance (Case 1)

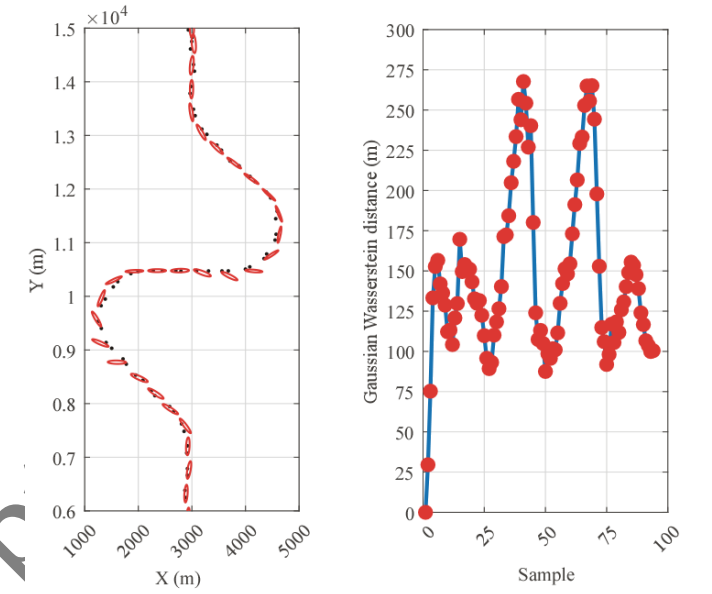

(b) Selecting shorter dwell time for Low Probability of Intercept (LPI) (Case 2)

Figure 10: Group Target Tracking (a) $T_d = 0.5$, (b) $T_d = 3.5$

Accepted Manuscript

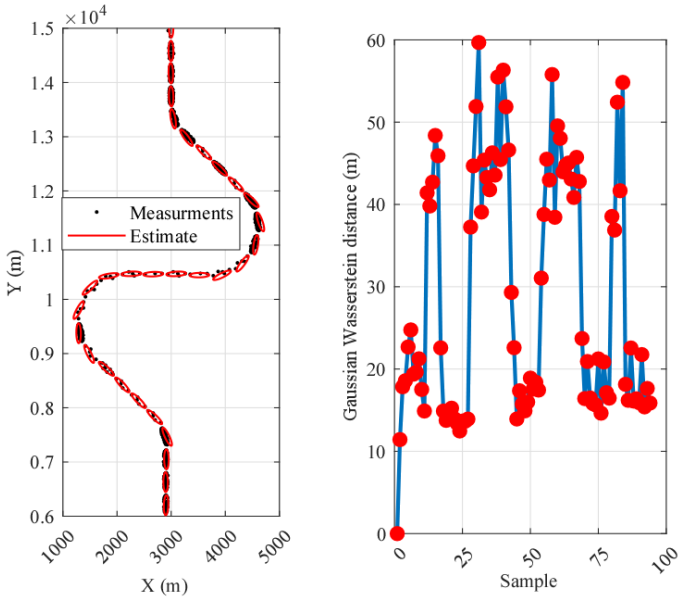

Figure 11: Group Target Tracking with Optimal Dwell Time Allocation (Case 4)

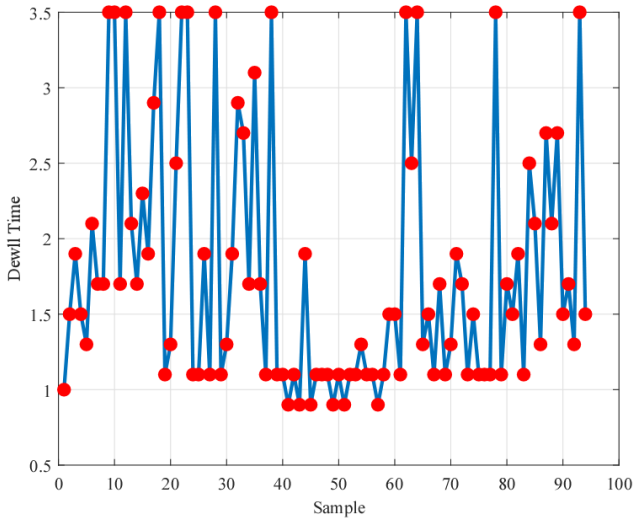

Figure 12: Optimal Dwell Time for Group Target Tracking

Accepted manuscript

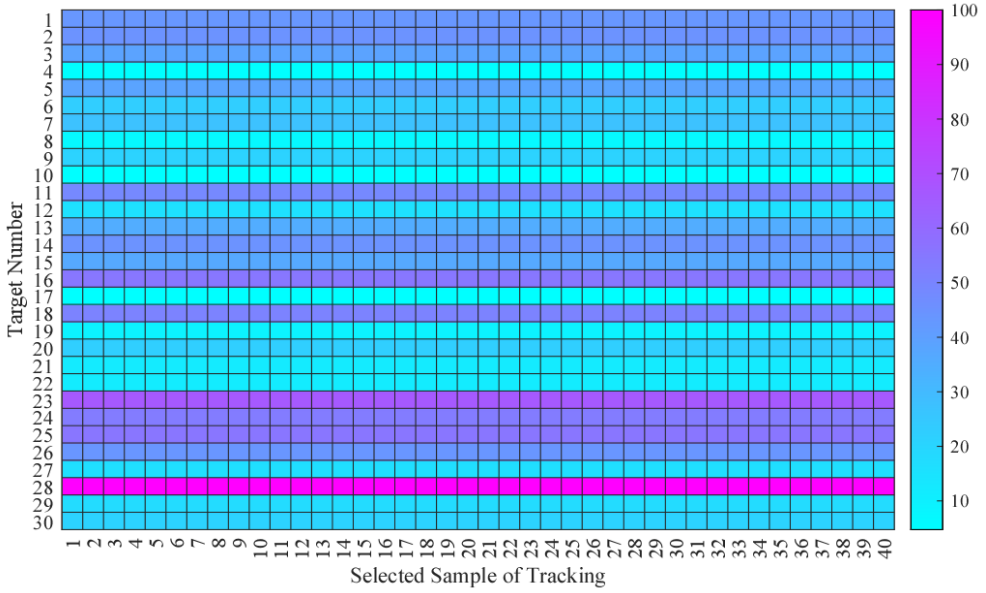

Figure 13: Resource Consumption in optimized dwell time allocation for MTT approach (Scaled)

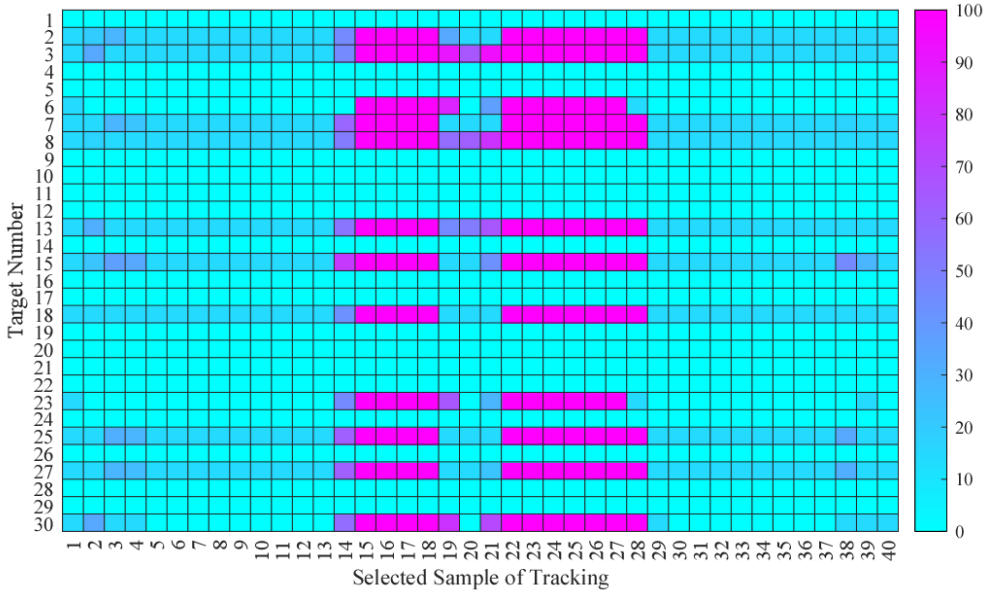

Figure 14: Resource Consumption in Optimal Dwell Time Allocation for Group Target Tracking (Scaled)

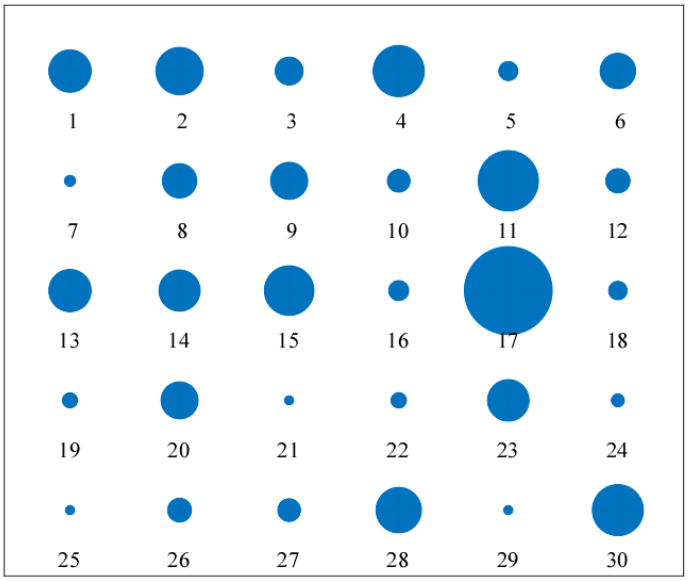

Figure 15: Participation of Targets in optimized dwell time allocation for MTT approach

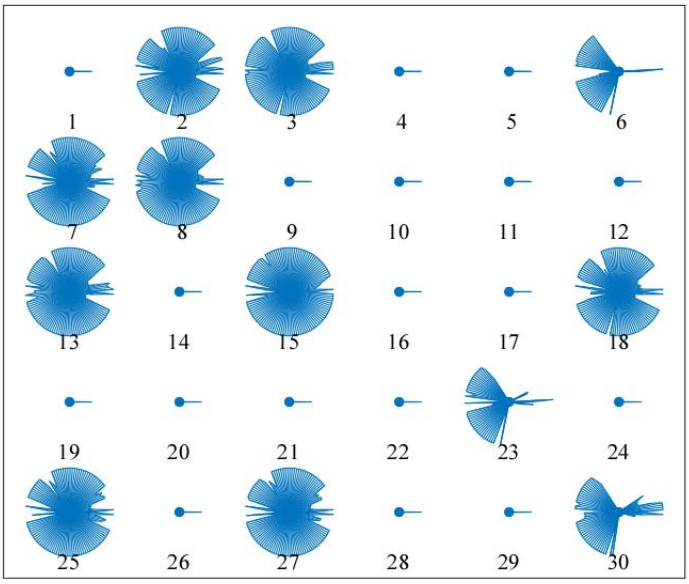

Figure 16: Participation of Targets in Optimal Dwell Time Allocation for Group Target Tracking

Accepted manuscript

Tables

Table 1: pseudo code of tracking with optimal dwell time
Initiation;
For each track do

| Prediction (kienematic & geometry parameters);
| Radar detection procedure with allocated Td;
| If detection associated with track then
| | Update Track with observations ;
| end
| Solve Eq. (58);
| Send Td to Radar management unit
| Adapte radar radiation with Td
End

Table 2: Comparison of Various Dwell Time Allocation Approaches in Group Target Tracking

Dwell Time	Mean GW Error	STD GW Error	Time Consumption	Cost
$T_d = 0.5$	113.05	19.62	94	**893**
$T_d = 1$	61.33	14.17	376	**115**
$T_d = 1.5$	38.30	12.77	2397	**134**
$T_d = 2$	38.25	12.01	9588	**102**
$T_d = 2.5$	26.22	15.08	19975	**93**
$T_d = 3.5$	22.35	16.86	32900	**97**
T_d^{opt} in MTT	23.38	15.7	15930	**95**
T_d^{opt} in GTT	29.15	15.01	6674	**91**

Accepted by Scientia Iranica

Biographies

Essmaeel Zamani

Phd. candidate

Affiliation
Faculty of Electrical & Computer Engineering

Malek Ashtar University of Technology

Tehran, Iran

Publication Topics

Tracking, Group Traget, Estimation, Resource Management, Control, Optimal, Multivariable, MIMO, Robust, Radar, Tracker, Nonlinear Control, Observer, Neural network, Adaptive control, Cramer-Rao Lower Bound, Fisher Information Matrix, Covariance Matrix, Control Method, Sliding Mode.

Biography

Essmaeel Zamani was born in Markazi, Iran, in 1980. He obtained a B.S. in Electronics Engineering from Arak Azad Islamic University in 2003 and an M.S. in Control Engineering from the Islamic Azad University, Science and Research Branch, Tehran, in 2005. He is currently a PhD candidate at Malik Ashtar University. His research interests encompass the design of tracking systems, signal and data processing, control systems, and estimation. Since 2006, he has been affiliated with the Department of Electrical and Computer Engineering at Malek Ashtar University of Technology.

Dr. Seyyed Mohammad Mehdi Dehghan

Associate Professor

Also published under: Seyyed M. Mehdi Dehghan, S. M. Mehdi Dehghan

https://www.orcid.org/0000-0002-3835-0212

Affiliation
Faculty of Electrical & Computer Engineering

Malek Ashtar University of Technology

Tehran, Iran

Publication Topics

Tracking, Group Target, Allocation, Line-of-sight, Path Loss, Cramer-Rao Lower Bound, Fisher Information Matrix, assignment, Local Approach, Localization Accuracy, Non-line-of-sight, Path Loss Model, Multi Target, Radiofrequency, Received Signal Strength, Rescue Missions, Actuator Faults, Ad Hoc Networks, Adaptive Sliding Mode Control, Angle Of Arrival, Angular Position, Angular Velocity, Attitude Control System, Chief Complaint, Control Method, Control Problem, Covariance Matrix, Direct Signal, Distance Estimation, Effects Of Obstacles.

Biography

Seyyed Mohammad Mehdi Dehghan was born in Tehran, Iran, in 1977. He received a B.S. degree in computer engineering in 1999, an M.S. in Artificial Intelligence and robotics engineering in 2002, and a Ph.D. in control

engineering in 2011 from Tehran University, Tehran, Iran. His research interests include tracker design, estimation, and machine learning. Since 2014, he has been with the electrical and electronic engineering department of Malek Ashtar University of Technology, Tehran, Iran. He is the director of the Control and Robotics Research Institute at Malek Ashtar University.

Dr. Iman Mohammadzaman*

* Corresponding author

Associate Professor

Affiliation
Faculty of Electrical & Computer Engineering

Malek Ashtar University of Technology

Tehran, Iran

Publication Topics

Optimization, convex optimization, Non convex optimization, uncertainty, Robust, Gain-scheduling, Localization Accuracy, Line-of-sight, Proportional Guidance, Guidance Law, Non-line-of-sight, State-space, Nonlinear control, Density function, Rescue Missions, Actuator Faults, autopilot, Adaptive Sliding Mode Control, Angle Of Arrival, Angular Position, Angular Velocity, Attitude Control System, Parametric uncertainty, Control Method, Control Problem, Covariance Matrix, Direct Signal, Distance Estimation, Parametric uncertainty, State-space Stability

Biography

Iman Mohammadzaman received his Ph.D. degree in control engineering from Tarbiat Modares University, Tehran, Iran, in 2011. Since 2013, he has been an Associate Professor with the Faculty of Electrical and Computer Engineering, Malek Ashtar University of Technology, Tehran, Iran. His research interests include robust control, nonlinear control, and convex optimization.

Dr. Reza Fatemi Mofrad

Associate Professor

Affiliation
Electrical & Computer Engineering Department

K. N. Toosi University of Technology

Tehran, Iran

Publication Topics

Antenna Array, Phased Array,Phased Array Radar, Sidelobe,Sidelobe Level, Amplitude Error, Angle Measurements, Aperture,Array Pattern, Azimuth Angle,Beamwidth,Broad Beam,Coverage Of Space,Detection Probability,Dielectric Constant Of The Substrate,Gain Margin, Half-power Beamwidth, Least Mean Square, Linear

Array,Maximum Efficiency, Methods For More Details, Microstrip Patch, Mutual Coupling, Narrow Beam, Narrow Beamwidth

Biography

Reza Fatemi-Mofrad was born in Tehran, Iran, in 1974. He received a B.S. in electronics engineering from Sharif University of Technology, Tehran, Iran in 1998, an M.S. in telecommunications engineering from Tehran University in 2001, and a Ph.D. in telecommunications engineering from K. N. Toosi University of Technology, Tehran, Iran in 2011. His research interests include radar systems design, Signal And Data processing. Since 2011, he has been with the electrical and electronic engineering department of Malek Ashtar University of Technology, Tehran, Iran.

Accepted by Scientia Iranica